AMEGHINIANA
A GONDWANAN PALEONTOLOGICAL JOURNAL

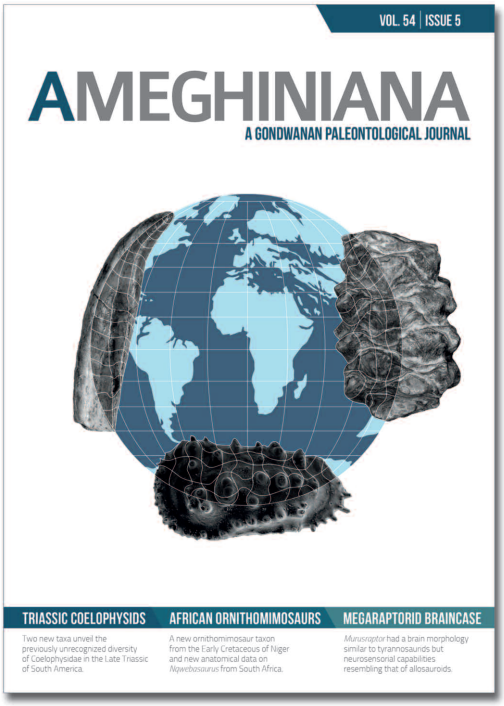

A THEROPOD DINOSAUR FROM THE LATE JURASSIC CAÑADÓN CALCÁREO FORMATION OF CENTRAL PATAGONIA, AND THE EVOLUTION OF THE THEROPOD TARSUS

OLIVER W. M. RAUHUT[1]
DIEGO POL[2]

[1]SNSB, Bayerische Staatssammlung für Paläontologie und Geologie, Department of Earth and Environmental Sciences, GeoBioCenter, Ludwig-Maximilians-University, Richard-Wagner-Str. 10, 80333 München, Germany.
[2]CONICET, Museo Paleontológico Egidio Feruglio, Av. Fontana 140, U9100GYO Trelew, Argentina.

Submitted: April 4th, 2017 - **Accepted:** October 12th, 2017 - **Published online:** November 1st, 2017

To cite this article: Oliver W.M. Rauhut, and Diego Pol (2017). A theropod dinosaur from the Late Jurassic Cañadón Calcáreo Formation of central Patagonia, and the evolution of the theropod tarsus. *Ameghiniana* 54: 506–538.

To link to this article: http://dx.doi.org/10.5710/AMGH.12.10.2017.3105

ISSN 0002-7014
AMEGHINIANA - 2017 - Volume 54 (5): 539 – 566
GONDWANAN PERSPECTIVES

A THEROPOD DINOSAUR FROM THE LATE JURASSIC CAÑADÓN CALCÁREO FORMATION OF CENTRAL PATAGONIA, AND THE EVOLUTION OF THE THEROPOD TARSUS

OLIVER W. M. RAUHUT[1], AND DIEGO POL[2]

[1]SNSB, Bayerische Staatssammlung für Paläontologie und Geologie, Department of Earth and Environmental Sciences, GeoBioCenter, Ludwig-Maximilians-University, Richard-Wagner-Str. 10, 80333 München, Germany. *o.rauhut@lrz.uni-muenchen.de*

[2]CONICET, Museo Paleontológico Egidio Feruglio, Av. Fontana 140, U9100GYO Trelew, Argentina. *dpol@mef.org.ar*

Abstract. A fragmentary postcranial skeleton from the Late Jurassic (Oxfordian–Tithonian) Cañadón Calcáreo Formation of Chubut, Argentina, represents a new taxon of theropod dinosaur, which is here described as *Pandoravenator fernandezorum* gen. et sp. nov. This material represents the first Late Jurassic theropod known from Argentina. *Pandoravenator fernandezorum* is characterized by strongly elongated postzygapophyses in the caudal vertebrae and an unusual tarsal joint, with the astragalus showing two distal tubercles and a very low and laterally inclined ascending process. Phylogenetic analyses indicate that the new taxon is a basal tetanuran, although its exact phylogenetic position within basal tetanurans remains uncertain, due to the fragmentary nature of the remains and the lack of consensus among the different phylogenetic analyses. The tarsus of *P. fernandezorum* shows an intermediate morphology between that of basal theropods and more derived tetanurans. It is especially noteworthy for the presence of a suture between the distal astragalar condyles and the anteroproximal extension of the astragalus, including the ascending process. This indicates that a separate ossification of the ascending process of the astragalus was present in this taxon, and, in a phylogenetic context, thus provides evidence that the origin of the ascending process and the astragalar body from separate ossifications was already present at the base of Averostra.

Key words. Theropoda. Tetanurae. Jurassic. Tarsals.

Resumen. UN DINOSAURIO TERÓPODO DE LA FORMACIÓN CAÑADÓN CALCÁREO DEL JURÁSICO TARDÍO DE PATAGONIA CENTRAL, Y LA EVOLUCIÓN DEL TARSO DE LOS TERÓPODOS. Un esqueleto postcraneano fragmentario de la Formación Cañadón Calcáreo del Jurásico Tardío (Oxfordiano–Titoniano) de Chubut, Argentina, representa un nuevo taxón de dinosaurio terópodo, el cual es descripto aquí como *Pandoravenator fernandezorum* gen. et sp. nov. Este material representa el primer terópodo conocido del Jurásico Tardío de Argentina. *Pandoravenator fernandezorum* se caracteriza por sus postzigapófisis caudales fuertemente alargadas y una articulación tarsal inusual, con el astrágalo mostrando dos tubérculos distales y un proceso ascendente muy bajo e inclinado lateralmente. Diversos análisis filogenéticos indican que el nuevo taxón es un tetanuro basal, aunque su posición precisa dentro de los tetanuros basales permanece incierta debido a la condición fragmentaria de los restos y la falta de consenso en los diferentes análisis filogenéticos del grupo. El tarso de *P. fernandezorum* muestra una morfología intermedia entre la de los terópodos basales y tetanuros más derivados. Es especialmente destacable la presencia de una sutura entre los cóndilos distales y la extensión anteroproximal del astrágalo, incluyendo el proceso ascendente. Esto indica que este taxón poseía un centro de osificación separado en el proceso ascendente del astrágalo, y en un contexto filogenético, podría proveer evidencia de que el origen del proceso ascendente a partir de un centro de osificación separado ocurrió en la base de Averostra.

Palabras clave. Theropoda. Tetanurae. Jurásico. Tarso.

ALTHOUGH recent phylogenetic analyses indicate that most major lineages of theropod dinosaurs reach back to the Jurassic (*e.g.*, Choiniere *et al.*, 2010; Rauhut *et al.*, 2010; Xu *et al.*, 2010; Pol and Rauhut, 2012; Carrano *et al.*, 2012; Rauhut *et al.*, 2016), our understanding of Jurassic theropod evolution is largely based on the fossil record from the Northern Hemisphere (Rauhut and López-Arbarello, 2008). For the Late Jurassic, the only Gondwanan unit that has yielded identifiable remains is the Tendaguru Formation of southern Tanzania, from where a number of ceratosaurian and basal tetanuran taxa are known (Janensch, 1920, 1925, 1929; Rauhut, 2005a, 2011; Rauhut and Carrano, 2016). In South America, Late Jurassic theropods have so far only been reported from the Tithonian Toqui Formation of southern Chile, from where Salgado *et al.* (2008) described fragmentary remains that were recently referred by Novas *et al.* (2015) to the highly unusual basal tetanuran *Chilesaurus*. The latter represents the only formally named possible

theropod taxon from the Late Jurassic of South America; however, it should be noted that its theropod affinities are disputed, as *Chilesaurus* has recently been re-interpreted as an ornithischian (Baron and Barrett, 2017).

The Oxfordian–?Tithonian Cañadón Calcáreo Formation of Chubut Province, Argentina, has yielded numerous dinosaur remains in recent years, mainly representing sauropods. Theropods seem to be rare in this formation, but several fragmentary specimens have been found in the past 15 years. Here we describe a new taxon of theropod from a new locality, Caja de Pandora, located on the western banks of the Río Chubut, some 12 km north of the village of Cerro Cóndor. The new taxon is interpreted as a basal tetanuran and bears peculiar features in the tarsus that have implications for understanding the evolution of the astragalus and its ascending process in Theropoda.

GEOLOGICAL AND PALAEONTOLOGICAL SETTING

The Caja de Pandora locality (Fig. 1) is situated in the outcropping area of the Cañadón Calcáreo Formation, some 1000 m west of the fish locality of Puesto Almada (López-Arbarello *et al.*, 2013), in the middle course of the Río Chubut, Chubut Province, Argentina. The Cañadón Calcáreo Formation is a unit of terrestrial sediments that were deposited in the Cañadón Asfalto Basin, a large, north-northwest–south-south-east trending depocenter in northern central Chubut Province (Figari and Courtade, 1993; Figari, 2005). It represents the post-rift phase of the basin (Figari and Courtade, 1993; Figari, 2005; Figari *et al.*, 2015) and comprises a mainly lacustrine basal part, followed by fluvial and overbank deposits. A tuff at the top of the lacustrine section at Puesto Almada has recently been dated at 157 Ma (latest Oxfordian; Cúneo *et al.*, 2013). The section at this locality has been referred to as Puesto Almada Member of the Cañadón Asfalto Formation by other workers (*e.g.*, Cabaleri *et al.*, 2010; Gallego *et al.*, 2011; Volkheimer *et al.*, 2015), but, despite the differences in nomenclature, there is agreement in the Late Jurassic age of these rocks (Cabaleri *et al.*, 2010).

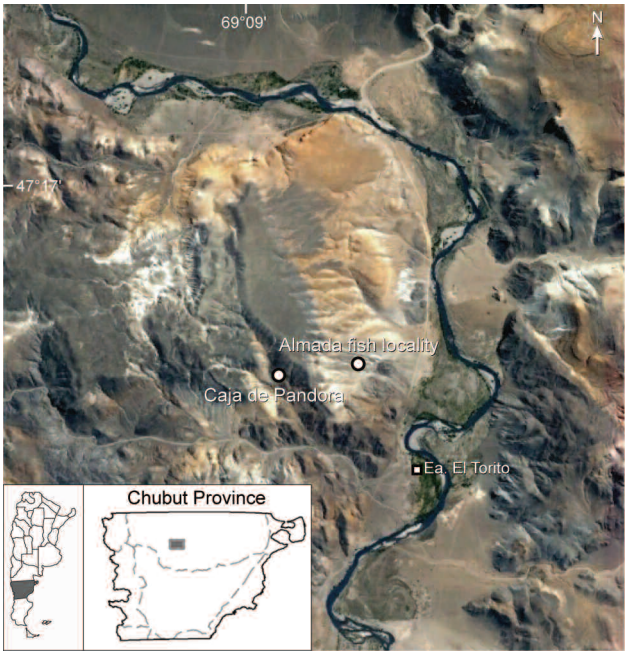

Figure 1. Satellite image showing the Caja de Pandora locality in the Puesto Almada area, west of the Chubut river in central Chubut Province, Argentina. Abbreviation: *Ea.*, Estancia.

Due to faulting, the section in which the Caja de Pandora locality is placed cannot directly be correlated with the Puesto Almada locality, since there is only a restricted outcrop of the Cañadón Calcáreo Formation in this area, and much of the outcrop is covered by debris from Miocene basalts that cap the formation on top. However, parts of the outcropping sediments at the locality consist of fine-grained, laminated sandy siltstones, which are similar to intercalated lacustrine levels in the transition between the lacustrine and fluvial part of the section at Puesto Almada, and thus we consider it very likely that these sediments represent this part of the section. Thus, the age of this locality probably very closely corresponds to the radiometric date obtained at Puesto Almada (for further discussion of the geology of the Cañadón Calcáreo Formation see Figari, 2005; Cúneo *et al.*, 2013; López-Arbarello *et al.*, 2013; Figari *et al.*, 2015).

In 2002, a fieldwork team of the Museo Paleontológico Egidio Feruglio, led by one of us (OR), discovered two distal caudal vertebrae, articulated with their chevron at Caja de Pandora. The remains were collected from the surface, and an intensive search of the area by the whole team in the next day recovered additional caudal vertebral fragments, but failed to identify the exact level and location where these remains came from. In January 2009, the senior author again visited the site, and a number of additional fragments, mainly of hindlimb elements, were found. Again, an

intensive search led to the recovery of a few more bones, but no remains could be found *in situ*. Finally, the distal part of a left tibia, an astragalus and a few other fragments (including remains of two articulated pedal phalanges) were found by DP in 2017. Despite the disparate times of discovery, all elements were found in the same erosional gully in an area of six to eight square meters. Furthermore, the recovered elements are of matching size, preservational quality, and, in the case of bones known from both left and right side, of matching morphology (allowing for some deformation), so that all of this material seems to represent a single individual. The hindlimb elements found in 2009 were recovered from an even more restricted area of some two square meters, further strengthening the interpretation that at least these remains belong to the same animal.

Vertebrate remains have been found *in situ* at the Caja de Pandora locality in a hard, silicified layer of laminated fine sandstone of some 50 cm thickness, which is brown to dark red in colour. Fossils found in this layer were mainly fish (*Luisiella* sp.) and isolated unidentified bones. Although the preservation and attached sediment of the theropod bones agree with the characteristics of this layer, no theropod remains could be discovered *in situ*, and all remains were found some 5 m below this layer.

Apart from these remains, the Cañadón Calcáreo Formation has yielded an abundant fish fauna from the basal lacustrine part (the Almada fauna; López-Arbarello *et al.*, 2008), including the coccolepid *Condorlepis groeberi* (Bordas, 1943; López-Arbarello *et al.*, 2013) and the basal teleost *Luisiella feruglioi* (Bordas, 1943; Bocchino, 1967; Sferco, 2012; Sferco *et al.*, 2015), as well as the basal crocodyliform *Almadasuchus*, found towards the top of the lacustrine section at Puesto Almada (Pol *et al.*, 2013), the sauropod dinosaurs *Tehuelchesaurus* (Rich *et al.*, 1999; Carballido *et al.*, 2011) and *Brachytrachelopan* (Rauhut *et al.*, 2005), an unidentified brachiosaurid (Rauhut, 2006), and a diplodocid (Rauhut *et al.*, 2015).

Institutional Abbreviations. **FMNH,** Field Museum of Natural History, Chicago, USA; **MB,** Museum für Naturkunde Berlin, Berlin, Germany; **MCNA,** Museo de Ciencias Naturales y Antropológicas (J. C. Moyano), Mendoza, Argentina; **MOR,** Museum of the Rockies, Bozeman, USA; **MPEF,** Museo Paleontológico Egidio Feruglio, Trelew, Argentina.

SYSTEMATIC PALEONTOLOGY

DINOSAURIA Owen, 1842
THEROPODA Marsh, 1881
TETANURAE Gauthier, 1986

Pandoravenator fernandezorum gen. et sp. nov.
Figures 2–8

Etymology. From Pandora, referring to the type locality 'Caja de Pandora' and *venator*, Greek for hunter. The species name honours the Fernandez family, including Daniel Fernández and the late Victoriano Fernández and his daughters and sons (especially Abel). The family has helped in many ways the exploration of the Museo Paleontológico Egidio Feruglio on their land in the Upper Jurassic rocks of central Chubut for more than twenty years.

Holotype. MPEF PV 1773-3, distal end of right femur and proximal end of right tibia; 1773-6, proximal end of right fibula; 1773-5a, b, fragment of the proximal shaft of the left tibia and proximal sections of the shafts of the right tibia and fibula; 1773-4, distal end of articulated right tibia, fibula, astragalus and calcaneum; 1773-7, partial right distal tarsal 4; 1773-8, proximal end of right metatarsal IV; 1773-9, articulated left distal tarsals 3 and 4 and proximal ends of metatarsals II to IV; 1773-10, articulated distal ends of right metatarsals II to IV, proximal ends of phalanges II-1 and IV-1, and ungual of digit I; 1773-11, distal end of left metatarsal II; 1773-12, distal end of left metatarsal III; 1773-13-17, fragments of five pedal phalanges; 1773-18, pedal ungual; 1773-27–28, mid-shaft of a slender long bone (?fibula).

Referred material. MPEF PV 1773-21, fragments of two articulated distal mid-caudal vertebrae; MPEF PV 1773-19, one-and-a-half distal caudal vertebrae with articulated chevron; MPEF PV 1773-20, parts of two articulated distal caudal vertebrae; MPEF PV 1773-2, glenoid region of left scapulocoracoid; MPEF PV 1773-1, distal end of left humerus; MPEF PV 1773-36, fragment of the distal end of the left tibia (MPEF PV 1773-36a) and articulated partial left astragalus (MPEF PV 1773-36b); MPEF PV 1773-37, fragments of two articulated pedal phalanges.

Comments. Although we consider all of the material to represent a single individual (see above), we restrict the holotype

to the hindlimb elements in order to avoid confusion in case future discoveries demonstrate that remains of more than a single individual or taxon are present at this locality. As noted above, the discovery of the hindlimb elements at the same time in a very restricted spot and the fact that all of these elements are of matching size and repeated elements (mainly metatarsals and distal tarsals) are of matching morphology leave little doubt that at least these remains represent the same animal. The very fragmentary scapulocoracoid (MPEF PV 1773-2) and distal humerus (MPEF PV 1773-1) were found at the same time as the hindlimb elements just a few meters below the latter within an erosional gully; their preservation and the slightly further displacement indicate that these elements might have eroded out some time earlier. Their size is consistent with that of the hindlimb elements. The caudal vertebrae found in 2002 (MPEF PV 1773-19–21) were recovered from the same general area (as noted above, within a 6–8 m^2 range) and, as far as this can be established, their size is within the range expected for an animal of the size represented by the hindlimb elements; the referral of these remains should thus be seen as somewhat more tentative. The fragmentary tibia (MPEF PV 1773-36a), astragalus (MPEF PV 1773-36b) and phalanges (MPEF PV 1773-37) recovered in 2017 are eroded and seem to be deformed. Nevertheless, the elements were again found in the same small area and the discernible morphology matches that of the holotype of *Pandoravenator*.

Type locality and horizon. Caja de Pandora locality, *ca.* 1 km west of the fish locality of Puesto Almada, Chubut Province, Argentina (Fig. 1). The material was found in a section of lacustrine and fluvial silt to sandstones that can be referred to the basal part of the Cañadón Calcáreo Formation, latest Oxfordian to Kimmeridgian.

Diagnosis. Small to medium-sized theropod dinosaur that can be diagnosed by an astragalus with anterior and distal lateral tubercles adjacent to the contact with the calcaneum, an anteriorly facing part of the astragalar body that is offset from the distal part by a transverse groove anteriorly, an ascending process of the astragalus that is laminar, but very low (about one third of the height of the astragalar body), triangular in outline in anterior view, and inclined laterally, and the shaft, but not proximal end, of metatarsal III being strongly constricted between the shafts of metatarsals II and IV. A further potential apomorphy, based on the referred material, is the postzygapophyses of posterior caudal vertebrae being elongate to overhang approximately half of the length of the following vertebral centrum.

DESCRIPTION

Caudal vertebrae

Most of the recovered posterior caudal vertebrae are poorly preserved, but MPEF PV 1733-19 (Fig. 2) and MPEF PV 1733-20, both of which include the remains of two articulated posterior caudal vertebrae and are reasonably well-preserved, provide information on the morphology of these elements. The fact that both include strongly elongated posterior caudal vertebrae, but are derived from different parts of the caudal column, as evidenced from their quite different sizes, indicates that the tail of *Pandoravenator* was long and slender.

MPEF PV 1733-19 represents the more anterior section of the posterior tail. The more anterior of the two caudal vertebrae preserved in articulation is almost complete, with only minor parts of the anterior end missing, whereas the more posterior element is only represented by its anterior half. The vertebral centra are elongate, with the anterior vertebra being 56 mm long (with an additional 1–2 mm missing at the anterior end) and 18 mm high posteriorly. The vertebral body is slightly wider than high (21 vs. 18 mm at the posterior end), notably constricted ventrally (to a minimal height of approximately 12 mm in the anterior vertebra), but only slightly transversely (minimal width is 16 mm). Due to the articulated state of all vertebral fragments found, the exact shape and nature of the articular ends cannot be established, although they seem to be amphi- to platycoelous. A weakly-developed, but notable lateral longitudinal ridge is present at about midheight of the vertebral body, and the ventral side of the vertebra is offset from the lateral sides by notable edges, giving the centrum a hexagonal outline in cross-section, as in many basal tetanurans. The ventral surface between these edges is flat to very slightly concave transversely. The posterior end of the centrum extends slightly further ventrally than the anterior end to form the chevron facets. These seem to be developed as small, separate, posteroventrally directed facets in the more anterior vertebra, where they are partially hidden by the articulated chevron.

On the lateral side, the ventral margin of the basis of the massive prezygapophysis extends posteroventrally to the midlength of the centrum, where it reaches half of its height (Fig. 2.1–2), as in the posterior caudal vertebrae of the noasaurid *Elaphrosaurus* (Rauhut and Carrano, 2016), the basal tetanuran *Allosaurus* (Madsen, 1976) and basal coelurosaurs, such as ornithomimosaurs (*e.g.*, Osmólska *et al.*, 1972). Anteriorly, it is developed as a stout, rounded ridge, which becomes more indistinct posteroventrally and, at its posteroventral end, is separated from the longitudinal lateral ridge of the centrum by a shallow, narrow, slightly curved groove. The broken posterior end of the more posterior vertebra shows the hollow interior of the centrum, surrounded by bone walls of *ca.* 4 mm laterally and 2 mm ventrally, and apparently devoid of internal septa or trabeculae.

The neural arch extends over almost the entire length of the centrum, its base being separated from the anterior margin of the latter by some 5 mm and from its posterior end by 9 mm. It is low, being approximately 12 mm high above its posterior base, and encloses a small, round neural canal. The prezygapophyses are massive and strongly elongated, the elements of the more posterior vertebra of MPEF PV 1773-19 extending over *ca.* 37 mm or approximately 65% of the length of the preceding vertebra (Fig. 2), as in *Allosaurus* (Gilmore, 1920; Madsen, 1976) and many coelurosaurs (*e.g.*, Osmólska *et al.*, 1972), but in contrast to the generally shorter posterior caudal prezygapophyses in *Ceratosaurus* (Gilmore, 1920; Madsen and Welles, 2000) and non-averostran theropods. The prezygapophyses are more anteriorly than dorsally directed, in contrast to the more strongly dorsally inclined prezygapophyses in *Majungasaurus* (O'Connor, 2007). The base of the prezygapophysis of the more posterior vertebra is 11 mm high at its highest point, just above the anterior end of the centrum, where its ventral margin also shows a notable lateral bulge in dorsal view. Anteriorly, the tongue-shaped prezygapophyses narrow to a point. The ventral margins of the prezygapophyses are generally more massive than the dorsal rims, which are developed as thin laminae and are narrowly spaced, being 6 mm apart posteriorly and 3 mm towards their anterior ends in the more posterior vertebra of MPEF PV 1773-19 (Fig. 2.3).

The bases of the prezygapophyses extend posteriorly to about the midlength of the centrum, where their dorsal margins merge into the roof of the neural arch. In this area, the neural arch extends slightly dorsally towards the base of the postzygapophyses. Although the exact morphology of the latter is difficult to establish, due to the fully articulated preservation, the postzygapophyses seem to be placed on a long, single, rod-like posterior process that extends posteriorly to about the half-length of the following verte-

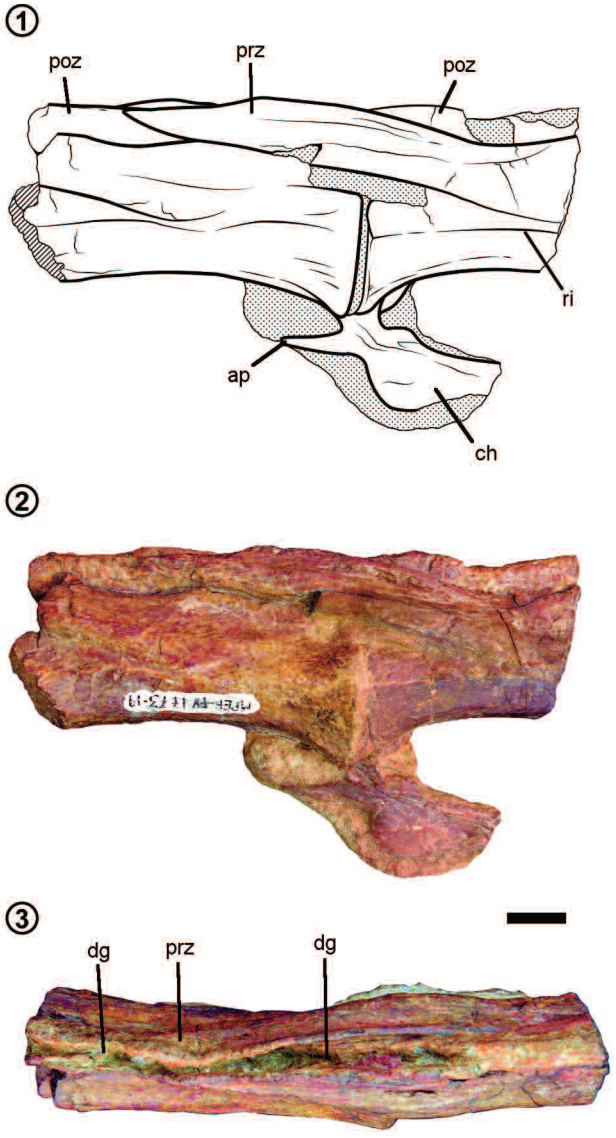

Figure 2. Caudal vertebrae of ***Pandoravenator fernandezorum***, **MPEF PV** 1733-19; **1–2,** outline drawing and photograph in left lateral view; **3,** photograph in dorsal view. Abbreviations: **ap,** anterior process; **ch,** chevron; **dg,** dorsal groove; **prz,** prezygapophysis; **poz,** postzygapophysis of the preceding vertebra; **ri,** lateral longitudinal ridge on the vertebral centrum. Scale bar= 10 mm.

bral centrum. There is no neural spine, but the dorsal side of this rod-like process is excavated by a narrow, but deep longitudinal groove (Fig. 2.3), as in *Condorraptor* (Rauhut, 2005b) and *Allosaurus* (Madsen, 1976).

Two articulated fragments of probably posterior middle caudal vertebral centra (MPEF PV 1773-21) show a convex ventral surface and a hollow interior of the centrum, but otherwise do not provide any useful morphological information. The more posterior caudal vertebrae MPEF PV 1773-20 are closely comparable to, but less well-preserved than the vertebrae described above. The lateral longitudinal ridge and the chevron facets are less distinctive than in the more anterior vertebrae, and, with an anterior width of 14 mm and a height of *ca.* 16 mm, the vertebral body is slightly higher than wide.

Haemapophysis

A single haemapophysis is preserved in articulation with the caudal vertebrae of MPEF PV 1733-19. It is almost complete, missing only the distalmost tip. The haemapophysis is dorsoventrally short and anteroposteriorly expanded distally, as in *Allosaurus* (Madsen, 1976) and other basal tetanurans. Whereas the anterior expansion and most of the ventral border are rounded, the larger posterior expansion seems to have been pointed, but its tip is broken off. Proximally, the expansion is separated from the slender articular processes for the vertebrae by a marked, angular "shoulder" posteriorly, and the anterior process anteriorly, the presence of which represents a theropod synapomorphy (Rauhut, 2003). The dorsal margin of the anterior process is aligned with the dorsal margin of the posterior "shoulder". The anterior process is more elongated than in *Allosaurus* (Madsen, 1976) and tapers to a sharp point anteriorly.

Pectoral girdle

The glenoid region of the left scapulocoracoid is preserved (MPEF PV 1773-2). Although scapula and coracoid are preserved in articulation, they are not fused, the suture between the two elements being well visible on both medial and lateral sides (Fig. 3). Unfortunately, the fragment is too incomplete to say anything about the general shape of the scapulocoracoid, but some details of the glenoid and its surrounding areas are discernible.

The broken base of the scapular blade is oval in cross-section, narrowing posteriorly. It is rather massive, being 13 mm wide transversely at the widest part. The medial side of the scapula bulges medially towards the glenoid, although the exact extent of this bulge cannot be established, since the surface of the bone is abraded in this area. On the lateral side, a well-developed lateral lip is present at the posterior end of the glenoid facet (Fig. 3). Between the medial bulge and lip, the ventral surface just behind the glenoid forms a wide, triangular surface. Unlike the situation in most theropods, in which this area is transversely convex, this surface is flat, although this might be due to abrasion in this area. The scapular glenoid facet accounts for 14 mm of the total 24 mm of the glenoid. Unlike the situation in basal theropods, in which the glenoid facet is usually mainly anteroventrally directed, it is more laterally directed (Fig. 3.3), at an angle of approximately 40° from the vertical, similar to the condition in maniraptorans (Norell and Makovicky, 1999; Rauhut, 2003). The scapular glenoid facet is transversely widest at the level of the lateral lip posteriorly, where its width is approximately 15 mm, but narrows to 12 mm anteriorly, before it slightly expands again towards the contact with the coracoid. Thus, its lateral margin is markedly concave in ventral view (Fig. 3.3). At the suture with the coracoid, the glenoid is 14 mm wide. The scapular glenoid facet is both anteroposteriorly and transversely slightly concave. A shallow, oval depression is present on the lateral side of the scapula above the glenoid, between the lateral lip and the coracoid suture (Fig. 3.1). The coracoid suture extends dorsally and slightly anteriorly from the glenoid to approximately 11 mm above the lateral rim of the latter. Here, it curves posteriorly, more so on the medial side than on the lateral side, so that the suture is transversely oblique in the broken dorsal cross-section, with the coracoid extending further posteriorly medially than laterally. Some 20 mm above the glenoid, the suture flexes again dorsally and extends almost straight towards the dorsal break on the medial side.

Although only the glenoid region of the coracoid is preserved, the structure of the preserved parts indicates that it was relatively short anteroposteriorly, unlike the elongate coracoids of dromaeosaurids (Norell and Makovicky, 1999) and other maniraptorans. The coracoid is transversely widest at the glenoid, and narrows dorsally and anteriorly.

Towards the anteroventral end of the preserved part, the bone widens again, slightly more so medially than laterally, to form the basis of the broken ventral process of the coracoid. A weak oblique ridge on the lateral side of this expansion probably corresponds to the coracoid tubercle ('biceps tubercle'). The biceps tubercle is developed as an oblique ridge in other taxa, including *Allosaurus* (Madsen, 1976), but it is more prominent and triangular in basal theropods, such as *Coelophysis rhodesiensis* (Raath, 1977) and *Zupaysaurus* (Ezcurra and Novas, 2007). Between the expansion and the glenoid, the ventral margin of the coracoid forms a sharp edge, from which the lateral side of the bone gradually extends dorsally (Fig. 3); thus, a longitudinal groove, as it is present in some theropods, is absent in this region in *Pandoravenator*.

The glenoid facet of the coracoid is oval in outline and has a raised and considerably thickened lateral rim. Although the facet accounts for 10 mm of the complete glenoid along the longitudinal axis of the scapulocoracoid, its length along its oblique long axis is approximately 14 mm. It is oval in outline and up to 16 mm wide transversely. As in the scapular glenoid facet, the facet of the coracoid is somewhat posteroventrolaterally directed and is slightly convex transversely, so that its lateral parts are more strongly laterally oriented than the medial parts.

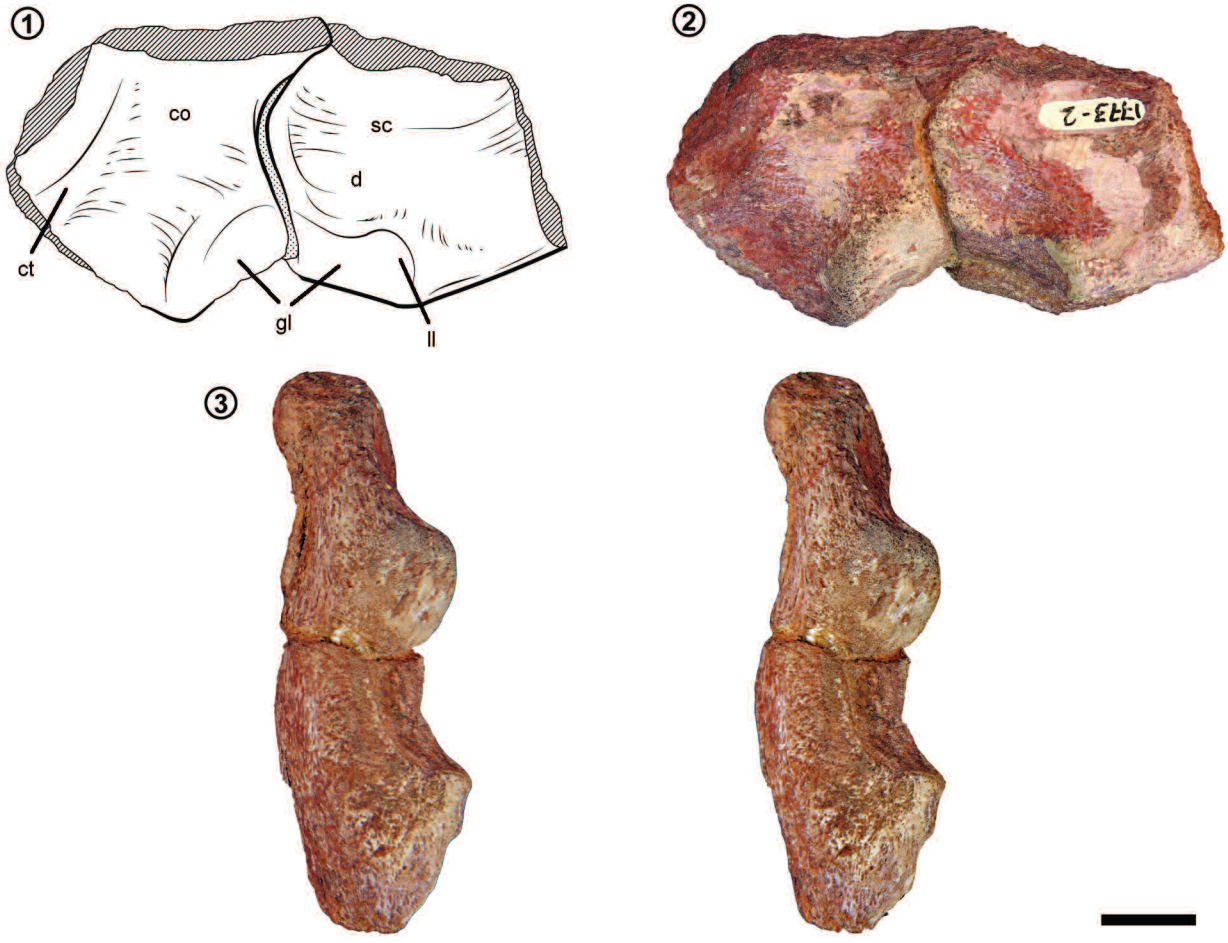

Figure 3. Left scapulocoracoid of ***Pandoravenator fernandezorum***, **MPEF PV** 1733-2; **1–2,** outline drawing and photograph in lateral view; **3,** stereophotograph in ventral view. Abbreviations: **co,** coracoid; **ct,** coracoid tubercle; **d,** depression; **gl,** glenoid; **ll,** lateral lip; **sc,** scapula. Scale bar= 10 mm.

Humerus

The distal end of the left humerus (MPEF PV 1773-1) is broken right above the distal condyles (Fig. 4), so nothing can be said about the shape of the humeral shaft. The distal end is, as preserved, 38 mm wide transversely. The medial, ulnar condyle is 15 mm deep anteroposteriorly, whereas the lateral, radial condyle measures 19 mm. The ulnar condyle is obliquely anteromedially-posterolaterally oriented, 22 mm wide transversely, and slightly widens anteroposteriorly from its lateral to its medial end (Fig. 4.2). The anteromedial expansion is mainly due to a stout, tubercle-like medial entepicondyle, which is largely eroded. The posterior side of the distal humerus is slightly concave between the entepicondyle and the lateral end of the ulnar condyle, which projects posteriorly. The distal articular surface of the ulnar condyle is slightly convex anteroposteriorly and more notably so transversely, so that the medial part extends slightly more proximally than the lateral part.

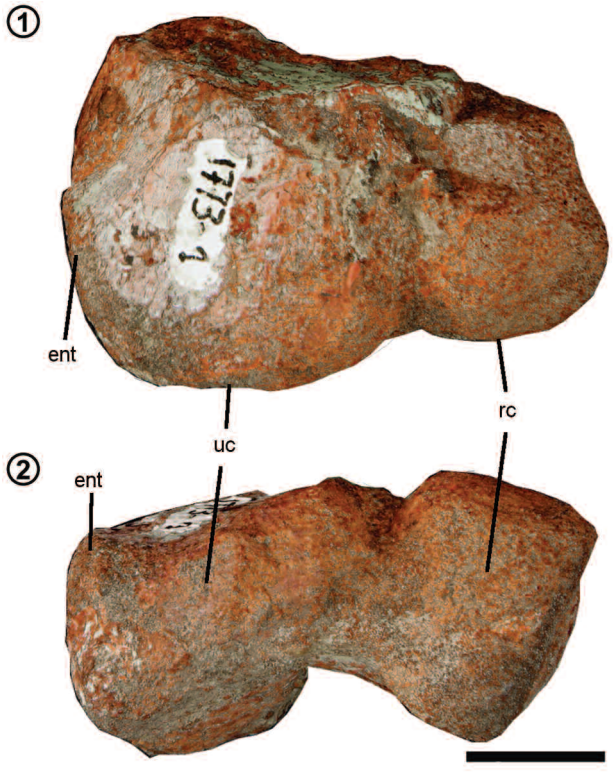

Figure 4. Distal end of left humerus of ***Pandoravenator fernandezorum***, **MPEF PV** 1733-1; **1,** photograph in anterior view; **2,** photograph in distal view. Abbreviations: **ent,** entepicondyle; **rc,** radial condyle; **uc,** ulnar condyle. Scale bar= 10 mm.

The ulnar condyle is separated from the radial condyle by a deep, broad, V-shaped incision posteriorly and a broad concavity distally (Fig. 4). The radial condyle has its long axis oriented anteroposteriorly, and is 19 mm wide in this direction and 14 mm transversely. It has a triangular outline in distal view, with a rounded anterior point (Fig. 4.2). Its distal articular surface is placed slightly more proximally than the lateral part of the ulnar condyle. It is almost flat anteriorly, only very slightly convex transversely, but extends in a convex arch onto the posterior side of the distal humerus posteriorly. The medial part of the articular surface on the posterior side of the humerus extends slightly more proximally medially than laterally, and thus forms the lateral border of the trough-like incision between the two condyles. The anterolateral side of the condyle is flat. On the anterior side of the distal humerus, there is a large depression laterally above the radial condyle and the lateralmost part of the ulnar condyle (Fig. 4.1). This depression gradually deepens from a broad ridge extending from the anterior point of the radial condyle proximally towards the medial side, and is bordered by a marked, slightly concave rim medially above the lateral part of the ulnar condyle. The exact extent of this depression cannot be established due to the proximal incompleteness of the bone. The lateral side of the distal end is notably flat, in contrast to the usually anteroposteriorly convex surface in most other theropods.

Femur

Only the distal end of the right femur is preserved (MPEF PV 1773-3; Fig. 5). A crystal infilled cavity is visible at the proximal break, indicating that the bone was hollow, as in most theropods. The shaft of the femur was oval to subtriangular in outline, but seems to be slightly deformed. As preserved, the distal end is 56 mm wide transversely, but a few mm might be missing at the anterolateral side of the eroded lateral condyle. A shallow, broad depression is present on the medial part of the anterior side of the distal part of the femur, as in many other theropods (Rauhut, 2003), but only its distalmost part is preserved. It is bound medially by a rounded, longitudinal medial edge on the anterior part of the medial side of the femur. This edge widens distally towards the distal condyle into a flat, triangular medial surface. However, in contrast to other theropods, such as *Allosaurus* (Madsen, 1976), *Megalosaurus* (Benson, 2010) and

Condorraptor (Rauhut, 2005b), this expansion is restricted to the distalmost part of the femur, and thus the resulting triangular area is wider anteroposteriorly than high proximodistally. The lateral part of the anterior side is convex transversely. The extensor groove on the anterior side of the femur was obviously very shallow or even absent, similar to the situation in *e.g. Dilophosaurus* (Welles, 1984), *Cryolophosaurus* (Smith *et al.*, 2007), and *Eustreptospondylus* (Sadleir *et al.*, 2008), but in contrast to many basal tetanurans, which usually have a well-developed extensor groove (*e.g.*, Madsen, 1976; Currie and Zhao, 1993; Rauhut, 2005b).

The distal condyles are strongly convexly rounded anteroposteriorly (Fig. 5). Only a slight concavity marks the distinction between the tibial and fibular condyles, but a small, moderately deep depression, which does not seem to be an artifact of preservation, is present in the central part of the articular end. The medial side of the distal end extends slightly further distally than the lateral side and both the tibial condyle and the *crista tibiofibularis* are inclined laterally (Fig. 5), though this might be exaggerated by deformation. The posterior expansion of the tibial condyle is subequal in size to the *crista tibiofibularis*, from which it is separated by a wide posterior intercondylar groove (Fig. 5.5). No infrapopliteal ridge is present, in contrast to coelophysoids and other basal theropods (Rowe, 1989; Tykoski, 2005). As in most theropods, the *crista tibiofibularis* is slightly offset from the distal end and from the lateral margin of the femur. A broad longitudinal depression is present between the fibular condyle and the crista laterally. There are two longitudinal ridges on the lateral side that extend from the distal condyle proximally. They are separated by *ca.* 7mm, and whereas the more posterior ridge ends at about the level of the proximal end of the *crista tibiofibularis*, the more anteriorly placed ridge extends some 10 mm further proximally.

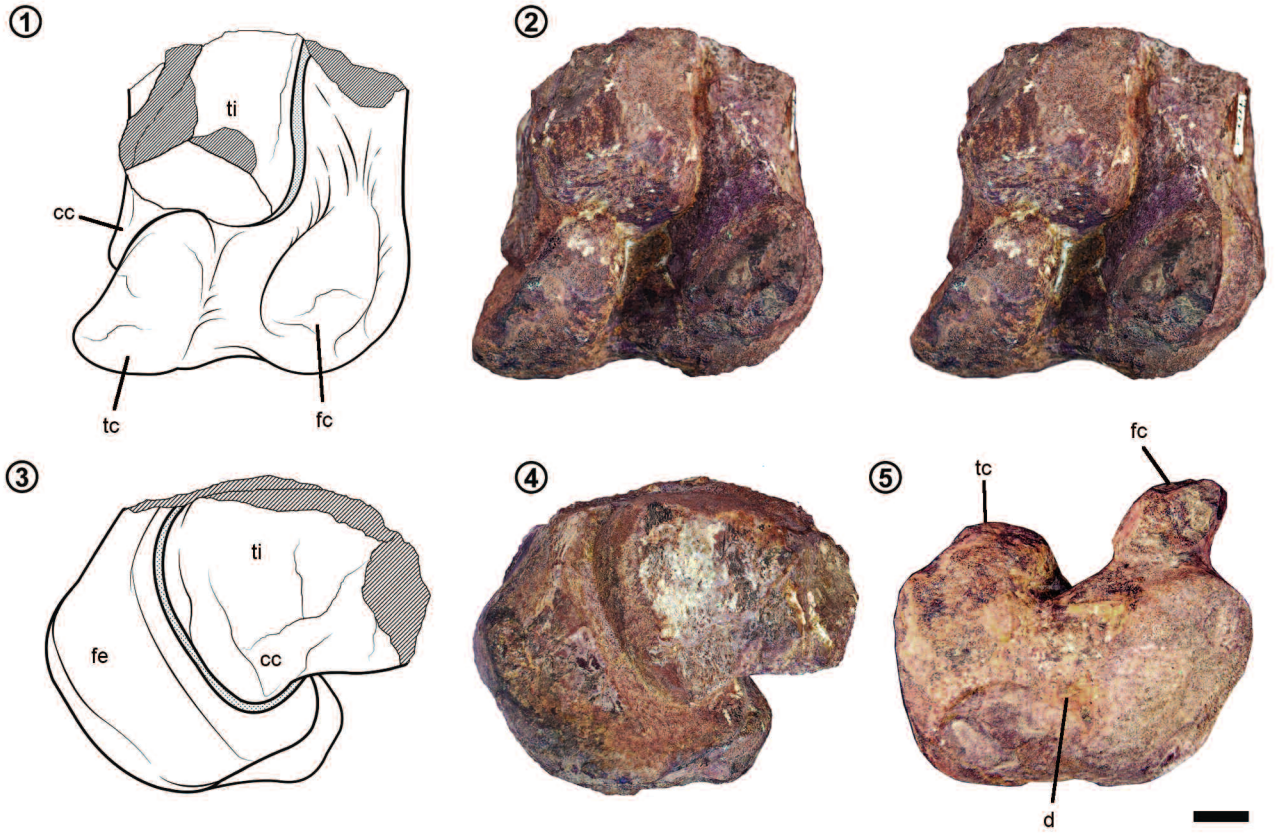

Figure 5. Distal end of right femur and proximal end of tibia of ***Pandoravenator fernandezorum***, **MPEF PV** 1733-3; **1–2,** outline drawing and stereophotographs in posterior view; **3–4,** outline drawing and photograph in medial view; **5,** photograph in distal view. Abbreviations: **cc,** cnemial crest; **d,** depression; **fc,** fibular condyle; **fe,** femur; **tc,** tibial condyle; **ti,** tibia. Scale bar= 10 mm.

Tibia

The tibia is represented by a fragment of the proximal part of the left shaft, a section of 96 mm of the proximal part of the right mid-shaft (MPEF PV 1773-5; Fig. 6), and the distal end of the left (MPEF PV 1773-36a) and right (MPEF PV 1773-4; Fig. 7) elements. Furthermore, a fragment of bone that is attached to the posteromedial side of the distal part of the femur probably represents the proximal end of the right tibia (Fig. 5.1–2). A part of the mid-shaft of the right fibula is preserved in articulation with the tibial shaft, and the distal end of the right tibia is articulated with the distal part of the fibula, astragalus and calcaneum.

As in the femur, the broken ends show that the tibia was hollow. If the interpretation of the fragment preserved with the femur as the proximal end of the right tibia is correct, the cnemial crest was rather small, anteriorly and very slightly proximally directed, and has a rounded anterior outline (Fig. 5.1, 4), similar to the condition in *Condorraptor* (Rauhut, 2005b), but unlike the usually much larger and more rectangular crest in ceratosaurs (*e.g.*, Gilmore, 1920; Madsen and Welles, 2000; Carrano *et al.*, 2002; Carrano, 2007; Rauhut, 2011; Pol and Rauhut, 2012; Rauhut and Carrano, 2016). In proximal view, there is no deeply-notched *incisura tibialis* separating the cnemial crest from the fibular condyle, but the former seems to extend rather gradually towards the latter structure, as in most non-tetanuran theropods (Rauhut, 2003). The posterior part of the proximal end is damaged, but a shallow, broad depression in the preserved part posteriorly, between the medial side of the proximal part of the tibia and the fibular condyle, indicates that a posterior incision between these two structures was present, as in most non-avian theropods (Rauhut, 2003).

Only a fragment of the proximal part of the shaft, showing the basis of the cnemial crest, is present for the left tibia. This fragment confirms that the cnemial crest was stout and its lateral side is only slightly concave towards the fibular condyle. There is no indication of any lateral ridge or crest connecting the proximal end with the fibular crest, as it is present in non-tetanuran theropods (Rauhut, 2003). The fibular crest is preserved in the section of the mid-shaft of the right tibia (Fig. 6). It is a stout lateral crest that distally gradually lowers into the shaft. Below the crest, the tibial shaft is broader transversely (33 mm) than anteroposteriorly deep (*ca.* 28 mm) and has a triangular

Figure 6. Proximal shaft of right tibia and fibula of ***Pandoravenator fernandezorum***, **MPEF PV** 1733-5; **1–2,** outline drawing and stereophotographs in anterior view. Abbreviations: **fc,** fibular crest; **fi,** fibula. Scale bar= 10 mm.

outline, with a flattened anterior side and a bulging posterior side. This posterior bulge becomes more pronounced proximally towards the proximal break. On the anterior side, a longitudinal depression seems to be present and becomes more conspicuous towards the distal break of the shaft, although it cannot be ruled out that this is due to deformation.

The distal end of the right tibia is generally well preserved (Fig. 7), but several details cannot be established because they are hidden by the articulated distal fibula and proximal tarsals. The distal end of the tibia is expanded transversely to a width of 67 mm and measures approximately 30 mm in anteroposterior direction, although the width might be slightly exaggerated by anteroposterior compression. Although covered by the proximal tarsals, the distal outline of the tibia is obviously broad and triangular, unlike the more rectangular outline in non-averostran theropods, but as in most non-maniraptoran averostrans (Rauhut, 2003). Whereas the medial malleolus is not notably expanded from the distal shaft, the lateral malleolus expands laterally into a rounded, lobe-like expansion that is directed laterally and slightly posteriorly and backs the distal end of the fibula posteriorly (Fig. 7.3–5). The morphology of the lateral malleolous is unlike the indistinct or more rectangular distal expansion seen in non-averostran theropods (*e.g.*, Ezcurra and Novas, 2007; Nesbitt and Ezcurra, 2015), or the gradual expansion in *Cryolophosaurus* (FMNH PR 1821; Smith *et al.*, 2007), *Elaphrosaurus* (Rauhut and Carrano, 2016), and *Ceratosaurus* (Madsen and Welles, 2000), but similar to the situation in *Piatnitzkysaurus* (Bonaparte, 1986), *Allosaurus* (Madsen, 1976), and *Tugulusaurus* (Rauhut and Xu, 2005), although the latter two taxa have a more pronounced medial expansion of the distal part of the tibia. In posterior view, the line of suture between the tibia and the astragalus is slightly sigmoidal, extending further proximally just distal to the anteroposteriorly broadest part of the distal part of the tibia, which is situated at approximately one third of the width of the bone from the medial side (Fig. 7.5). The lateral malleolus extends only very slightly further distally than the medial malleolus, unlike the situation in several basal tetanurans, including *Torvosaurus* (Britt, 1991) and carcharodontosaurids (Brusatte and Sereno, 2008), in which the latter extends notably further distally. On the anterior side of the distal part of the tibia, a pronounced step extends from the medial side laterally and slightly proximally and forms the proximal border of the attachment area for the astragalus (Fig. 7.1–2), as in most non-coelurosaurian basal averostrans (*e.g.*, Madsen, 1976; Britt, 1991; Currie and Zhao, 1993; Carrano, 2007), with the exception of noasaurids (Rauhut and Carrano, 2016). At about half the width of the bone, the step flexes proximally and extends almost vertically, only very slightly laterodorsally inclined, towards the proximal break. Here, the step has an anteroposterior depth of approximately 8 mm. The fragment of the distal end of the left tibia is strongly deformed and highly incomplete, providing no additional information.

Fibula

The proximal end of the right fibula (MPEF-PV 1773-6) lacks the posterior border of the bone and the shaft is broken some 50 mm below the proximal end. As in most theropods, the proximal end is kidney-shaped, but the transverse width remains subequal throughout the preserved part and does not get notably narrower posteriorly, as it is the case in most taxa. In lateral view, the proximal articular surface is slightly concave anteroposteriorly, with this concavity being mainly due to the presence of a small, rounded proximal expansion at the anterior end. With an estimated anteroposterior length of approximately 40 mm and a transverse width of 16 mm, the proximal end is rather robust. The lateral side of the proximal fibula is evenly convex anteroposteriorly, and the medial side gently concave. However, a deep medial groove is absent. Such a groove is present as a rather narrow, more posteriorly placed depression in most non-tetanuran theropods (*e.g.*, Rowe, 1989; Madsen and Welles, 2000; Carrano, 2007), and as a wide, deeply excavated groove with sharp margins in *Elaphrosaurus* (Rauhut and Carrano, 2016) and many tetanurans (Rauhut, 2003), with the notable exception of megalosauroids (Benson, 2010). Fine longitudinal striations are present on the surface of the medial side. Towards the distal break, the bone is deformed, so that the broken attachment of the shaft faces anterodistolaterally instead of distally.

A part of the mid-shaft of the right fibula is preserved in articulation with the tibia (MPEF PV 1773-5; Fig. 6). This includes the section that articulates with the fibular crest of

the tibia and slightly more distal parts of a total length of 56 mm. The proximal part of the preserved section is flattened transversely and slightly expanded anteroposteriorly to a width of 16 mm. There is no indication of the *iliofibularis* tubercle, which is found in this area in other theropods (*e.g.*, Currie and Zhao, 1993; Madsen and Welles, 2000; Brochu, 2003), and the posterior margin of the bone is more markedly thickened (*ca.* 9 mm) than the anterior edge (*ca.* 6

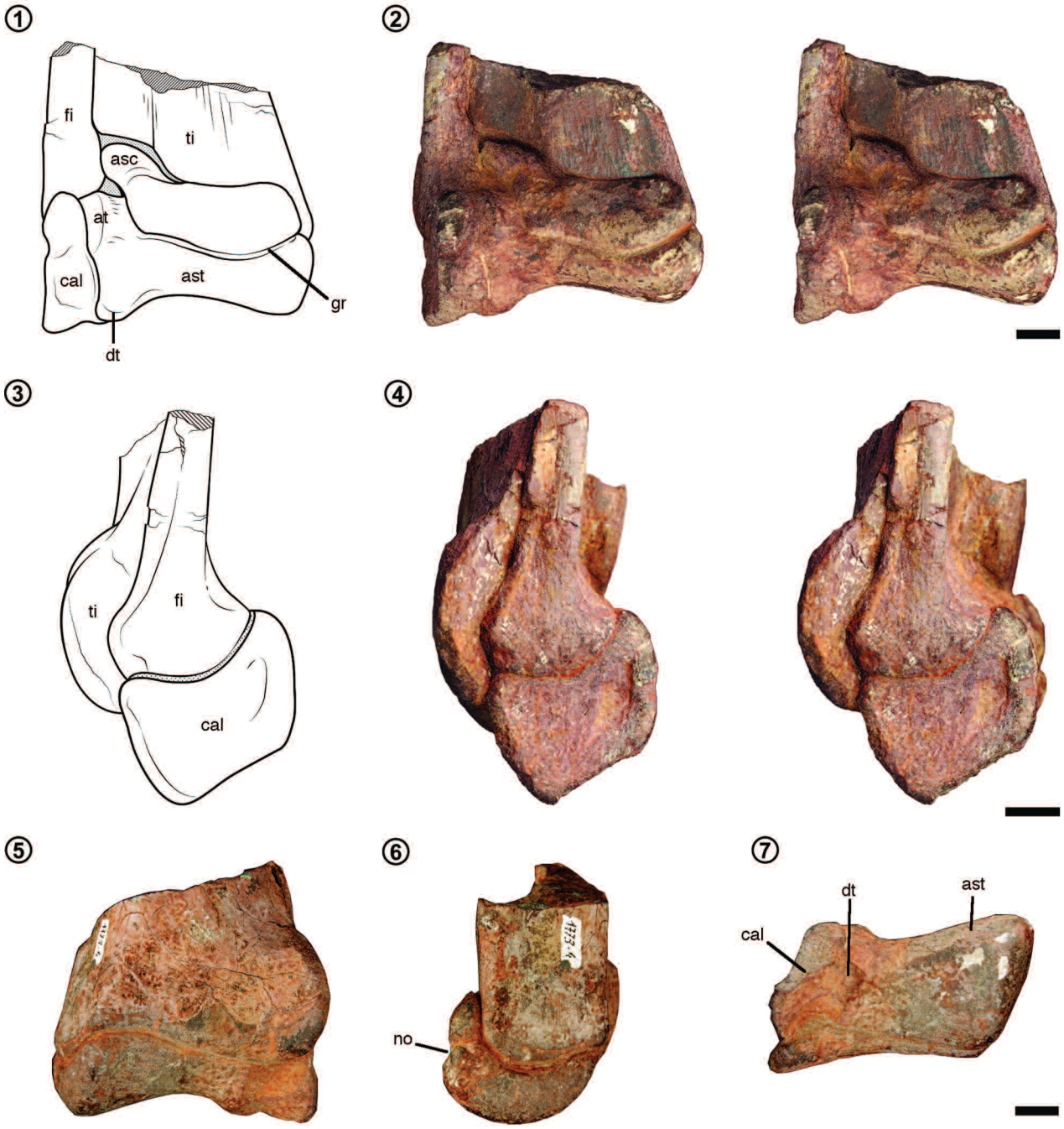

Figure 7. Distal end of right tibia, fibula, astragalus, and calcaneum of ***Pandoravenator fernandezorum***, **MPEF PV** 1733-4; **1–2,** outline drawing and stereophotographs in anterior view; **3–4,** outline drawing and stereophotographs in lateral view; **5,** photograph in posterior view; **6,** photograph in medial view; **7,** photograph in distal view. Abbreviations: **asc,** ascending process of astragalus; **ast,** astragalus; **at,** anterior tubercle; **cal,** calcaneum; **dt,** distal tubercle; **fi,** fibula; **gr,** groove; **no,** notch; **ti,** tibia. Scale bars= 10 mm.

mm). Below the insertion area of the *m. iliofibularis*, the fibula narrows slightly towards the distal shaft, and has an oval outline at the distal break, which is 10 mm wide anteroposteriorly and 8 mm transversely at the posterior margin. As in the more proximal section, the anterior margin is slightly thinner. The medial side of the fibula is convex anteroposteriorly and thus lacks a longitudinal depression, as it is found in some theropods (*e.g.*, Madsen, 1976).

The distalmost 42 mm of the right fibula is preserved in articulation with the tibia, astragalus and calcaneum (MPEF PV 1773-4; Fig. 7). At the proximal break, the bone is obliquely semioval with a very slightly transversely concave posteromedial side. It is approximately 11 mm wide anteroposteriorly and measures 7 mm in anterolateral-posteromedial direction. Distally, the bone rapidly expands, and the distal end has a maximal anteroposterior width of 26 mm. Whereas the posterior part of this expansion is triangular in lateral view (Fig. 7.3–4) and begins some 17 mm above the distal end, the anterior part is developed as an extensive bony lamina that gradually extends from approximately 35 mm above the distal end anterodistally (Fig. 7.1–2). This lamina is flexed medially in its anteriormost part and contacts the lateral side of the ascending process of the astragalus, as is the case in *Coelophysis rhodesiensis* (Rauhut, 2003: fig. 55A) and *Camposaurus* (Ezcurra and Brusatte, 2011). This morphology is notably different from that seen in most theropods, including non-averostrans, such as *Liliensternus* (Rauhut, 2003: fig. 55B), *Zupaysaurus* (Ezcurra and Novas, 2007), *Dilophosaurus* (Welles, 1984), ceratosaurs (*e.g.*, Madsen and Welles, 2000), and tetanurans (*e.g.*, *Allosaurus*: Madsen, 1976; *Sinraptor*: Currie and Zhao, 1993; *Eustreptospondylus*: Sadleir *et al*., 2008; *Tyrannosaurus*: Brochu, 2003), in which the expansion is less pronounced and the distal end is more robust. Although the suture between the fibula and the ascending process of the astragalus is tight, they are not fused, unlike the condition in adult abelisauroids (Carrano and Sampson, 2008) and at least some non-averostran theropods (*e.g.*, Nesbitt and Ezcurra, 2015). The distal articular surface of the fibula is strongly convex anteroposteriorly, facing distally at is posterior end and anterodistally at its anterior end (Fig. 7.3–4). The posterior margin of the fibula forms a small, posteriorly directed, triangular tubercle just above the distal articular surface.

Astragalus

The right astragalus and calcaneum are preserved in articulation with the tibia and fibula (MPEF PV 1773-4), and the medial half of the left astragalus (MPEF PV 1773-36b) has been preserved in articulation with a fragment of the distal left tibia. The astragalus is one of the most distinctive elements of *Pandoravenator*. It is a stout bone with the lateral side being considerably narrower anteroposteriorly than the medial side (Fig. 7.7), unlike the situation in *Liliensternus* (Rauhut, 2003: fig. 49B) and *Elaphrosaurus* (Rauhut and Carrano, 2016), but as in *Zupaysaurus* (Ezcurra and Novas, 2007) and tetanurans (*e.g.*, *Eustreptospondylus*: Sadleir *et al*., 2008; *Wiehenvenator*: Rauhut *et al*., 2016; *Allosaurus*: Gilmore, 1920; *Tyrannosaurus*: Brochu, 2003). The complete right element is parallelogram-shaped in distal outline, but the medial side of the left element shows that this might be partially due to anteroposterior compression, and the original shape might have been rather trapezoidal, narrowing laterally. The right astragalus measures approximately 47 mm transversely, is 33 mm wide medially, but only 28 mm wide laterally; whereas the transverse width might be slightly exaggerated, the anteroposterior measurements should be seen as minimal estimates, due to compression. The maximal proximodistal height of the right astragalus (excluding the ascending process) is 27 mm. In medial view, the distal astragalar body is kidney-shaped, narrowing posteriorly (Fig. 7.6). The medial side is almost flat proximodistally, but gently convex anteroposteriorly. A high, triangular (in medial view) part of bone is present proximal to the anteroproximal corner of the main astragalar body and is separated from the latter by a deeply incised notch in the right element (Fig. 7.6). This separation is only indicated by a shallow groove in the left astragalus. In the right astragalus, the anteroproximal expansion extends proximally for *ca.* 11 mm (13 mm in the left element) and articulates proximally with the step on the anterior side of the tibia, as in other non-coelurosaurian theropods. In anterior view of the right astragalus, the notch between the main astragalar body and the anteroproximal expansion extends laterally in a distally slightly convex arch as a well-developed, narrow, but deep and suture-like groove (Fig. 7.1–2). This groove ends some 10 mm medial to the contact with the calcaneum, where it turns sharply proximally and becomes a thin, slightly laterally inclined line

that extends towards the lateral margin of the ascending process of the astragalus. Both the groove and this line are reminiscent of a suture, but the clearly defined groove is absent in the left element, although its course can be followed as a fine line on the anterior side of the bone towards its lateral break. In the right astragalus, the proximal margin of this anteroproximally part of the bone follows the course of the distal border of the step on the anterior side of the tibia until the latter flexes abruptly proximally (as described above). From there, the margin expands into the ascending process of the astragalus. It first flexes steeply proximolaterally for approximately 6 mm and then extends much less steeply proximolaterally over 13 mm until it contacts the anteromedial margin of the fibula (Fig. 7.1–2). The lateral margin of the ascending process of the astragalus is inclined proximolaterally, so that the whole process has a slight lateral inclination, as in *Liliensternus* (Rauhut, 2003: fig. 49A), *Zupaysaurus* (Ezcurra and Novas, 2007), and *Ceratosaurus* (Madsen and Welles, 2000), but unlike the more vertical process in most tetanurans (*e.g.*, *Allosaurus*: Madsen, 1976). In total, the ascending process is very low (maximally 10 mm or 37% of the maximal height of the astragalar body, although 1–2 mm might be missing proximally due to erosion), laminar, but rather stout anteroposteriorly, and its base extends over only 13 mm, or approximately 28%, of the breadth of the astragalar body, being placed entirely on the lateral half of the latter. Apart from being laminar, the ascending process of *Pandoravenator* is comparable in height, width and placement, with that of many non-averostran theropods, such as *Liliensternus* (Rauhut, 2003) and *Zupaysaurus* (Ezcurra and Novas, 2007). Among ceratosaurs, which have a laminar ascending process, the position and placement of the process are comparable at least with those of *Ceratosaurus* (Madsen and Welles, 2000), *Elaphrosaurus* (Rauhut and Carrano, 2016) and abelisaurids (Carrano, 2007), although in the latter it seems to be higher.

The distal articular surface of the astragalus is strongly convex anteroposteriorly and is concavely arched in anterior view (Fig. 7.1–2). In posterior view, the tibia-astragalus contact extends further distally on the lateral than on the medial side. The astragalus is closely appressed, but not fused to the calcaneum. There are two large, unusual tubercles at the suture between the two elements. The larger of these is placed laterally at the anteroproximal end of the astragalar body, lateral to the base of the ascending process (Fig. 7.1–2). It is *ca.* 14 mm high proximodistally and semioval in outline. The second tubercle is placed laterally on the distal surface of the astragalus (Figs. 7.1–2, 8.7). It is triangular in outline, *ca.* 11 mm in length anteroposteriorly, and delimited anteriorly by a shallow, oval to rectangular depression on the distal surface, which is 8 mm long anteroposteriorly and 6 mm wide transversely. Unlike the condition in *Allosaurus* (Welles and Long, 1974; Madsen, 1976) and other tetanurans (*e.g.*, Britt, 1991; Currie and Zhao, 1993), there is no lateral notch in the anterolateral side of the distal surface of the astragalus for a medial process of the calcaneum (Fig. 7.1–2).

Calcaneum

The calcaneum (MPEF PV 1773-4) is a high, but thin disc of bone. Its maximal transverse width is approximately 13 mm, or 28% of the width of the astragalus, very similar to the ratio seen in *Elaphrosaurus* (Rauhut and Carrano, 2016) and *Sinraptor* (Currie and Zhao, 1993), whereas the width of the calcaneum is less than 20% of the width of the astragalus in coelurosaurs (*e.g.*, Kobayashi and Barsbold, 2005; Rauhut and Xu, 2005; Brusatte *et al.*, 2012). The anterodistal and posteromedial parts of the bone are damaged, so that the exact proximodistal height cannot be established, but it was about 31–33 mm. In lateral view, the proximal articular facet for the fibula is horizontal in its posterior half, but flexes steeply anteroproximally in its anterior half (Fig. 7.3–4). Thus, the anterior end of the calcaneum extends approximately 11 mm further proximally than the posterior end. On the lateral side, the fibular articular surface extends all the way to the posterior end of the astragalus, but a small articular facet for the tibia is present posteromedially of this surface on the calcaneum (Fig. 7.3–4). The lateral side of the calcaneal body is very slightly concave both anteroposteriorly (Fig. 7.7) and proximodistally, with a large, inverted teardrop-shaped depression present close to the anterior margin (Fig. 7.3–4), as in *Allosaurus* (Madsen, 1976), *Elaphrosaurus* (Rauhut and Carrano, 2016), and an astragalocalcaneum referred to *Aerosteon* (MCNA-PV-3139). This depression is 8 mm high proximodistally and maximally 5 mm wide anteroposteriorly. The distal articular surface of the calcaneum is partly damaged, but based on the preserved portion it seems to be strongly convex anteroposteriorly and slightly convex transversely.

Distal tarsals

The distal tarsals III and IV are preserved in articulation with the metatarsus of the left side (MPEF PV 1773-9), but the lateral half of the right distal tarsal IV (MPEF PV 1773-7) was found in isolation, together with the proximal end of the right metatarsal IV. Distal tarsal III is the smaller of the two distal tarsals, as in *Allosaurus* (Madsen, 1976), but unlike the situation in *Coelophysis bauri* (Padian, 1986), *Coelophysis rhodesiensis* (Raath, 1977), *Dilophosaurus* (Welles, 1984), tyrannosaurs (Lambe, 1917; Brusatte *et al.*, 2012), and *Deinonychus* (Ostrom, 1969), in which these bones are of similar size or distal tarsal III is larger than distal tarsal IV (*e.g.*, Padian, 1986); *Sinraptor* is somewhat intermediate in that the distal tarsal III is slightly smaller than distal tarsal IV (Currie and Zhao, 1993). It is rectangular to trapezoidal in outline, with rounded edges and caps the central part of metatarsal III and a small part of the lateral margin of metatarsal II (Fig. 8.5–6). There is no posterolateral expansion, as it is present in *Coelophysis* (Padian, 1986) and *Sinraptor* (Currie and Zhao, 1993). The bone is 21 mm long anteroposteriorly and maximally 25 mm wide transversely. It is proximodistally thin anteriorly, but thickens posteriorly, with the thickest part (*ca.* 5 mm) being the posteromedial corner (Fig. 8.3–4). The proximal surface is slightly transversely convex anteriorly, and notably convex anteroposteriorly posteriorly.

Distal tarsal IV is larger than distal tarsal III, also approximately trapezoidal in outline, and caps the proximal end of metatarsal IV (Fig. 8.5–6). In anterior view of the articulated left tarsus and metatarsus, the proximal end of metatarsal IV is placed slightly distal to the proximal ends of metatarsals II and III, so that the proximal surface of distal tarsal IV is level with the proximal surface of metatarsal III (Fig. 8.1–2). The long axis of distal tarsal IV is oriented anterolaterally-posteromedially, and it is 23 mm wide anteriorly, 29 mm long along its long axis, and approximately 14 mm wide posteriorly. The anteromedial corner of the bone is pointed, whereas the anterolateral edge is rounded and slightly raised, similar to the condition in *Allosaurus* (Madsen, 1976) and *Sinraptor* (Currie and Zhao, 1993). The anterior side between these two edges forms an almost straight line. The medial side of the bone marks a concave arch that contacts the lateral side of the anterior half of metatarsal III. The lateral margin of the distal tarsal is very slightly concave posterior to the rounded anterolateral edge, much less so than in many other basal theropods (Tykoski, 2005), but comparable to the condition of *Sinraptor* (Currie and Zhao, 1993). Posteriorly, the lateral corner of the bone is more broadly rounded than the medial edge, and the posterior margin between them is straight.

The proximodistal thickness of the bone varies considerably. The anteromedial part of the bone bulges distally to articulate with a corresponding depression in the proximal articular surface of metatarsal IV, and forms a high, triangular surface adjacent to metatarsal III in anterior view (Fig. 8.1–2). This anteromedial expansion reaches a thickness of 10 mm along the contact with metatarsal III in the left tarsus. The bone rapidly thins laterally to a minimal thickness of approximately 3 mm. The lateral edge is raised proximally to a thickness of 5.5 mm, so that the proximal articular surface is notably concave in its lateral part. The posterolateral part of the distal tarsal IV bulges distally to form a semioval expansion posteriorly at the contact between metatarsal IV and III (Fig. 8.3–4). This bulge reaches a maximal thickness of 9 mm. The disarticulated partial right distal tarsal IV demonstrates that the distal articular surface is saddle-shaped between the anterior and posterior distal expansions.

Metatarsus

The metatarsus is represented by the proximal ends of the left metatarsals II to V (MPEF PV 1773-9), which are preserved in articulation, the isolated proximal end of the right metatarsal IV (MPEF PV 1773-8), the articulated distal ends of right metatarsals II to IV (MPEF PV 1773-10), and the isolated distal ends of left metatarsals II (MPEF PV 1773-11) and III (MPEF PV 1773-12). Unfortunately, no complete metatarsal shaft is preserved, so nothing can be said about the length of the metatarsus. However, many of the broken shaft fragments clearly show that, as is the case with the other long bones, the metatarsals were hollow interiorly (Fig. 8.8). In the following description, the distal ends of metatarsals II and III are mainly described based on the isolated ends of the left elements; the right metatarsals confirm the observations based on these elements, although the shaft of especially the right metatarsal III is strongly deformed.

Metatarsal II has a large, semioval to subtriangular

proximal articular surface (Fig. 8.5). The long axis of the articular end is oriented anterolaterally-posteromedially. Thus, the proximal end is 35 mm long along its long axis, and measures maximally 22 mm perpendicular to it. The lateral margin seems to be very slightly convex anteroposteriorly, but is largely covered by the medial margin of distal tarsal III. The anterior and anteromedial margin of the bone form a gradual curve, whereas the posteromedial

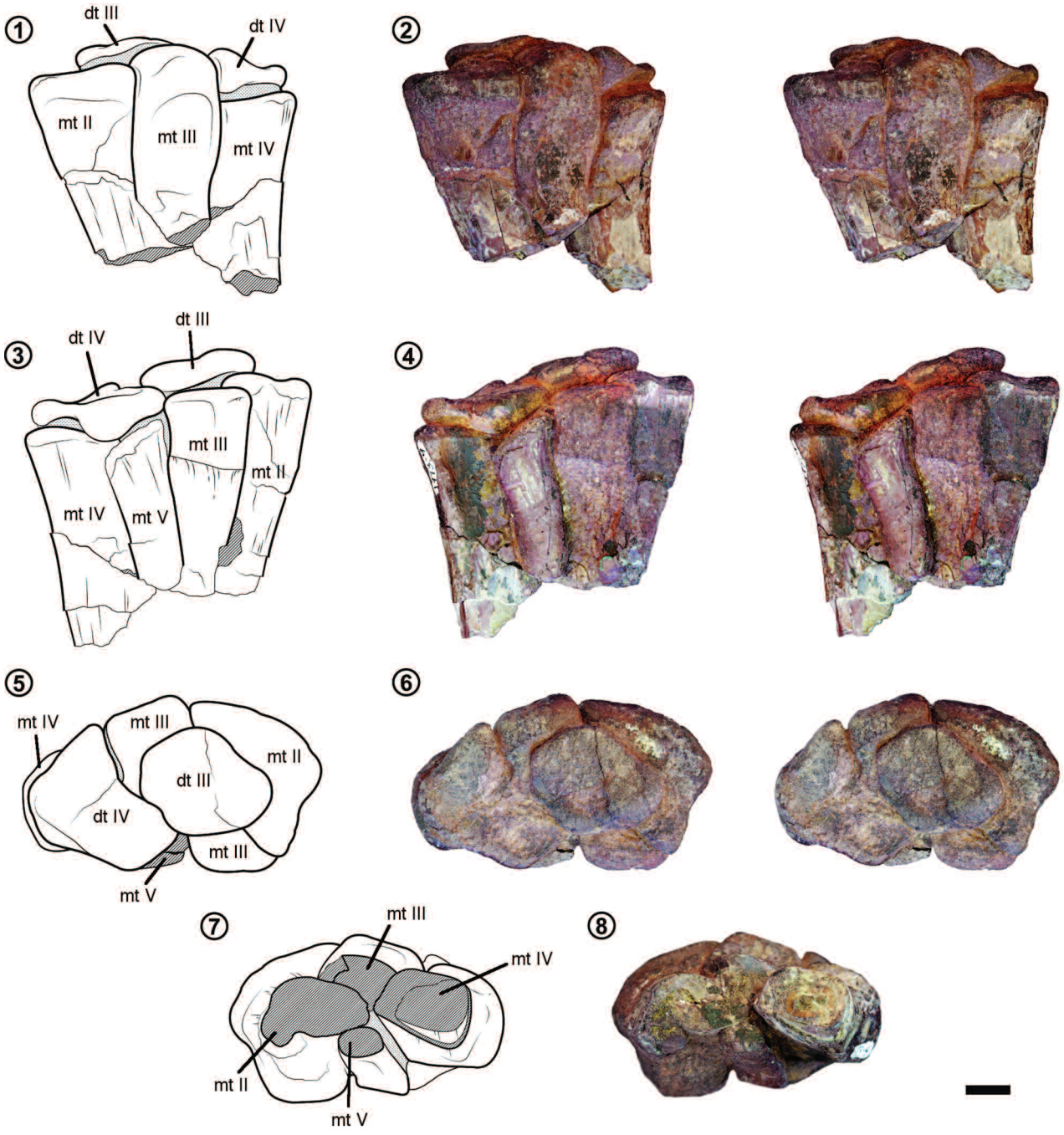

Figure 8. Articulated proximal left metatarsus and distal tarsals of ***Pandoravenator fernandezorum***, **MPEF PV** 1733-9; **1–2,** outline drawing and stereophotographs in anterior view; **3–4,** outline drawing and stereophotographs in posterior view; **5–6,** outline drawing and stereophotographs in proximal view; **7–8,** outline drawing and photograph in distal view showing the cross-section of metatarsals II-III-IV. Abbreviations: **dt,** distal tarsal; **mt,** metatarsal. Scale bar= 10 mm.

margin has a concave indentation (Fig. 8.5–6), as in *Ceratosaurus* (Gilmore, 1920), *Majungasaurus* (Carrano, 2007), megalosauroids (*e.g.*, Britt, 1991; Sadleir *et al.*, 2008), allosauroids (*e.g.*, Madsen, 1976; Currie and Zhao, 1993), and tyrannosaurs (Brochu, 2003), but unlike the convex margin in *Liliensternus* (Huene, 1934), *Coelophysis rhodesiensis* (Raath, 1977) and *Elaphrosaurus* (Rauhut and Carrano, 2016). This indentation is due to a small, triangular posterior flange that extends from the proximal shaft of metatarsal II posteriorly in lateral view. Apart from this posterior flange, the proximal end is more strongly expanded anteriorly than posteriorly. The shaft rapidly narrows, and is 16 mm wide anteroposteriorly and 13 mm mediolaterally at the distal break (45 mm below the proximal end). Here, the bone is anteromedially-posterolaterally flattened and has a semioval cross-section. The distal end of metatarsal II is stout and has a well-developed distal articular surface, which forms a round convex arch that extends over approximately 180° from the dorsal surface to the ventral surface of the bone (Fig. 9.8). There is no extensor groove on the dorsal surface of the bone, only the area adjacent to the distal articular surface shows a very weakly concave depression (Fig. 9.1–2, 5). A well-developed and deep collateral ligament fossa is present on the lateral side of the bone, separated by some 11 mm from the extremity of the distal end (Fig. 9.8). It is oval in outline and 10 mm long proximodistally and 6 mm high anteroposteriorly in the left metatarsal. A small, sharply defined, triangular lateral tubercle is present on the ventral margin of the lateral side, just below the anterior end of the collateral ligament fossa (Fig. 9.7). On the medial side, the collateral ligament fossa is only indicated by a large, but shallow depression adjacent to the distal articular surface (Fig. 9.6). The lateral side of the distal articular surface extends further distally than the medial side, so that the surface is inclined mediodistally at an angle of approximately 60° from the long axis of the shaft (Fig. 9.1–2, 5). The distal articular surface is transversely convex in its dorsal part, but subdivided into two distinct condyles in the ventral part (Fig. 9.7). These condyles diverge at an angle of approximately 65°, and the medial condyle is only about half the width of the lateral and tapers ventrally, whereas the lateral condyle is rounded. The lateral condyle is strongly transversely convex. At the proximal break, some 35–40 mm above the distal end, the shaft is oval in outline, with the long axis of the oval oriented slightly obliquely from anterolateral to posteromedial, and is approximately 16 mm wide transversely and 15 mm wide anteroposteriorly.

The proximal end of metatarsal III is hourglass-shaped in proximal view, as it is usual in basal tetanurans (*e.g.*, Madsen, 1976; Britt, 1991; Currie and Zhao, 1993), but unlike the elongate condition in *Dilophosaurus* (Welles, 1984), the T-shaped outline in *Ceratosaurus* (Gilmore, 1920) and *Elaphrosaurus* (Rauhut and Carrano, 2016), or the more blocky appearance in *Majungasaurus* (Carrano, 2007). The posterior end of the articular surface is displaced medially in comparison to the anterior end, and there seems to be a constriction between these ends, although most of this area is covered by distal tarsal III (Fig. 8.5–6). Furthermore, whereas the anterior margin faces mainly anteriorly, the posterior margin faces slightly posterolaterally. The articular surface is 17 mm wide anteriorly, 16 mm wide posteriorly, and 41 mm long anteroposteriorly. The anterior end bulges slightly proximally and the shaft rapidly narrows distally (Fig. 8.1–2). Whereas the anterior end fades into the shaft gradually, there is a large, rectangular tubercle posteriorly. This tubercle is 16 mm wide transversely, 14 mm high proximodistally, has a flat posterior surface, and is offset from the shaft by a distinct, concave step, similar to the situation found in *Allosaurus* (Madsen, 1976). At the distal break, some 42 mm below the proximal end, the posterior part of the shaft of metatarsal III is strongly pinched between the shafts of metatarsals II and IV, which almost meet posterior to metatarsal III (Fig. 8.7–8). It has the same inclination of the long axis as the proximal end and seems to be slightly constricted between the anterior and posterior sides. It is approximately 16 mm long anteroposteriorly, *ca.* 15 mm wide anteriorly and 13 mm wide posteriorly. The distal end of metatarsal III expands rapidly from a slender shaft. In the isolated left metatarsal (MPEF PV 1733-12), the shaft is compressed with a laterodorsally-ventromedially oriented long axis of the outline at the proximal break, some 60 mm proximal from the distal end. It is *ca.* 18 mm wide transversely and measures *ca.* 17 mm anteroposteriorly. The shaft is somewhat compressed posterolaterally-anteromedially, giving it an 8-shaped cross-section at the break, although this might be exaggerated by deformation. Just distal to the break, there is a small medial flange for the

contact with the distal metatarsal II. Thus, in articulation, the distal articular end of metatarsal II is placed entirely proximal to the expanded articular end of metatarsal III (Fig. 9.1–2, 5). The distal end of metatarsal III expands to a transverse width of 27 mm and an anteroposterior height of 25 mm medially and 21 mm laterally (Fig. 9.10). Collateral ligament pits are found on both the medial and lateral side of the distal end, but whereas the ligament pit on the medial side is developed as a moderately deep oval depression with a medially raised dorsal margin (Fig. 9.9), that of the lateral side is deeper and better defined, but also oval in outline (Fig. 9.11). The lateral collateral pit is approximately

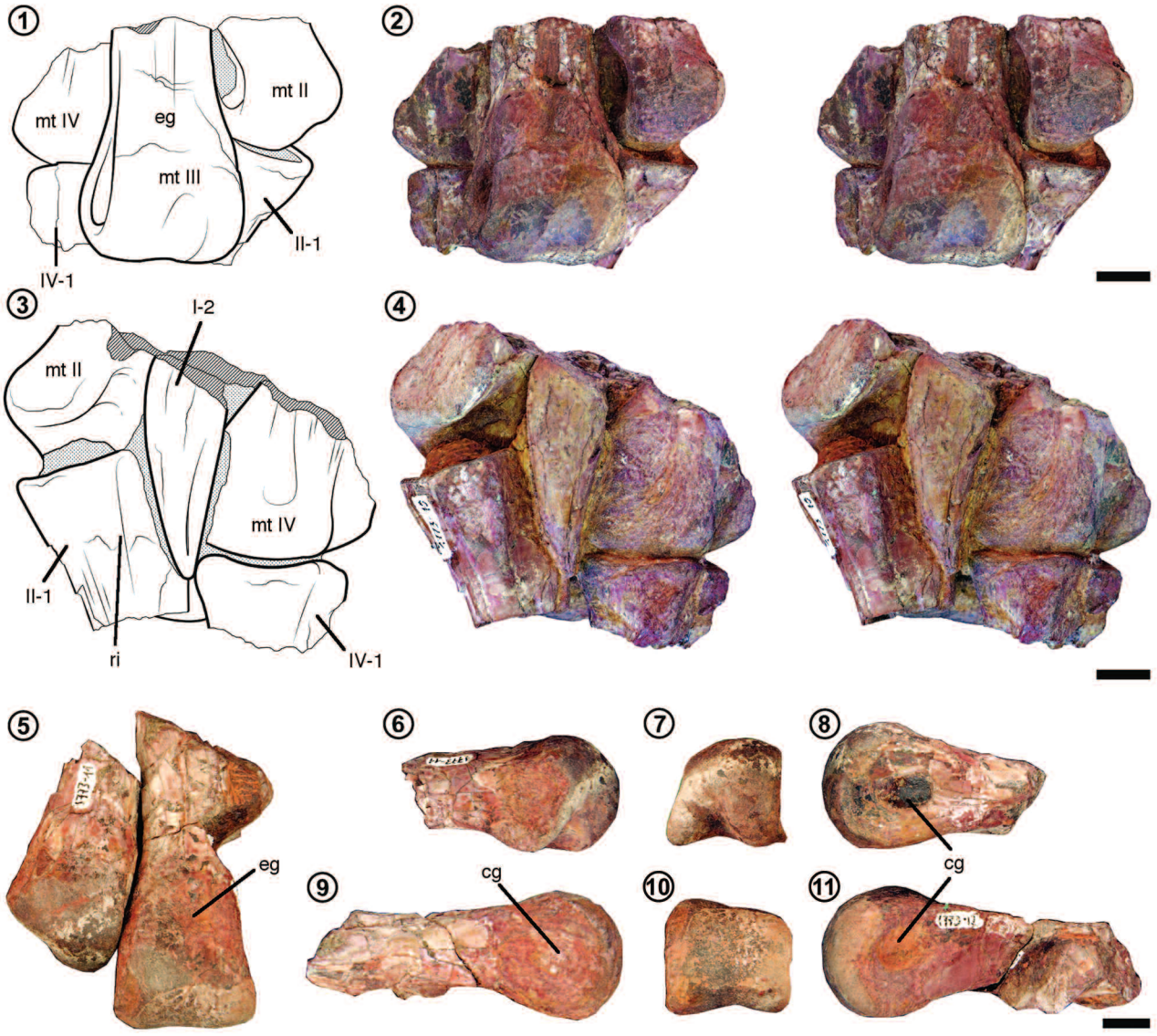

Figure 9. Distal end of metatarsals and proximal ends of pedal phalanges of ***Pandoravenator fernandezorum***. **1–4,** Outline drawing and stereophotographs of distal ends of right metatarsals II-III-IV, pedal ungual I, and phalanges II-1 and IV-1 (**MPEF PV** 1733-10) in **1–2,** anterior and **3–4,** posterior views; **5,** photograph in anterior view of left metatarsals II (**MPEF PV** 1733-11) and III (**MPEF PV** 1733-12); **6–8,** photographs of left metatarsal II (**MPEF PV** 1733-11) in **6,** medial, **7,** distal, and **8,** lateral views; **9–11,** photographs of left metatarsal III (**MPEF PV** 1733-12) in **9,** medial, **10,** distal, and **11,** lateral views. Abbreviations: **cg,** collateral ligament groove; **eg,** extensor groove; **mt,** metatarsal; **ri,** ridge; **I-2, II-1, IV-1,** pedal phalanges. Scale bars= 10 mm.

8 mm long proximodistally and maximally 7 mm high anteroposteriorly. On the anterior side of the distal end there is a small, rounded extensor groove, with a better-defined lateral than medial wall (Fig. 9.2). The groove is approximately 8 mm long proximodistally and 6 mm wide transversely, and is placed more on the lateral than on the medial side of the metatarsus. Just proximal to the thickened lateral edge of this groove, the bone narrows on the lateral side, forming a flat lateral surface for the contact with metatarsal IV. Thus, all three central metatarsals were obviously tightly appressed over their entire length. The distal articular surface of metatarsal III extends over an arc of approximately 180° from the anterior surface of the distal end to its posterior surface (Fig. 9.9, 11). It is broad, anteroposteriorly strongly convex, and subdivided into a slightly wider lateral and a narrower medial part by a very shallow transverse concavity (Fig. 9.10). Posteriorly, there are two small, widely diverging, flat condyles, separated by a very wide, V-shaped division.

The proximal end of metatarsal IV consists of a subround to subtriangular central articular surface and a long, posteromedially curved medial process at the posterior end, as it is usually found in tetanuran theropods. However, this process is broken off in the isolated proximal end of the right metatarsal IV and largely hidden by the articulated distal tarsal IV and metatarsal V in the left element, and not much can be said about its morphology. Only the distalmost tip can be seen in articulation with the posterolateral corner of metatarsal III. This tip shows that the distal extreme of the process tapers to a point. The proximal end of the left metatarsal IV is 21 mm long anteroposteriorly, 17 mm wide transversely anteriorly, and 33 mm wide posteriorly, including the posteromedial process. The lateral part of the proximal articular end is almost round in the left metatarsal (Fig. 8.1–4), but more triangular in the right element. The medial and posterior sides of this part form almost straight edges in both elements. The disarticulated right metatarsal IV shows that the proximal articular surface has a large depression anteriorly for the articulation with the distal tarsal IV, with slightly raised anterior and lateral edges. The shaft of metatarsal IV is only slightly constricted distally, with the main proximal expansions being anteriorly and, to a lesser extent, laterally. The posterior and medial sides of the shaft remain flat over the entire preserved length, and the posterior side is offset from the lateral side by a pronounced rounded edge. The anterior and lateral sides are also mainly flat, but curve into one another anterolaterally in a broad curve. Thus, at the distal break, the shaft of metatarsal IV is subrectangular in outline (Fig. 8.7–8), 20 mm wide transversely and 13 mm long anteroposteriorly. The distal end of the right metatarsal IV is preserved in articulation with metatarsals II and III and with a fragment of the first digit of the fourth toe (Fig. 9). Hence, some details of its morphology are difficult to establish. At the proximal break, the shaft of metatarsal IV is triangular in outline, with a flat medial and posterior surface, and a curved anterolateral side. The distal end is transversely narrow, expands considerably dorsoventrally from the shaft and is triangular in outline, tapering anteromedially. There are no collateral ligament grooves, but only a large, shallow depression on the medial side (Fig. 9.3–4), which is straight to slightly convex anteroposteriorly. The distal articular surface seems to be much more restricted than in metatarsals II and III, only slightly convex anteroposteriorly, and does not extend much onto the anterior and posterior sides of the bone (Fig. 9.4). It is subdivided in its posterior part into a broader medial condyle, and a narrow, widely diverging, posteriorly tapering lateral condyle. The distal end of the metatarsal is approximately 23 mm high anteroposteriorly and maximally 21 mm wide transversely. As in the case of metatarsal II, the distal articular end of metatarsal IV is placed entirely proximal to the distal articular end of metatarsal III (Fig. 9.1–2).

Metatarsal V is preserved in articulation on the posterior side of the posteromedial flange of metatarsal IV (Fig. 8.3–4), its proximomedial corner contacting the lateral side of the proximal posterior bulge of metatarsal III. Its proximal end is slightly damaged, and the distal end is broken off. The proximal end of the metatarsal is triangular in outline. It is 12 mm wide transversely, *ca.* 9 mm deep laterally, and tapers to a rounded point medially. The proximal surface steeply ascends from distolaterally to proximomedially, although this might partially be due to erosion. Towards the distal break, some 36 mm below the proximal end, the bone becomes slightly flattened, oval in outline and flexes very slightly laterally, as it is the case in many tetanuran theropods (Rauhut, 2003). The distal break is 10 mm wide transversely and 6 mm deep anteroposteriorly.

Pedal phalanges

Several fragments of pedal phalanges are preserved. The proximal ends of pedal phalanges II-1 and IV-1 are preserved in articulation with their respective metatarsals (Fig. 9.1–4). Phalanx II-1 is a stout element, 26 mm high and approximately 22 mm wide proximally. The proximal articular surface is concave, semioval in outline, with a flattened posterior side. On the medial side of the posterior (ventral) surface, a well-developed longitudinal ridge is present (Fig. 9.3–4). The ridge disappears some 22 mm distal to the proximal end and is separated from a pronounced posteromedial edge of the bone by a shallow depression proximally. At the distal break, the phalanx is oval in cross-section, with a slightly oblique long axis. A crystal-filled interior cavity shows that the phalanx was hollow, as is the case with all the other long bones of *Pandoravenator*. The pedal phalanx IV-1 has an asymmetric proximal end, fitting the distal articular surface of metatarsal IV. It is 21 mm wide and *ca.* 22 mm high. The proximal articular surface seems to have a semitriangular outline with a flat posterior side. Posteriorly, the proximal end of the phalanx is slightly concave transversely, mainly due to a pronounced, slightly posteriorly expanded lateral margin. Other fragments of proximal ends of pedal phalanges correspond closely to this morphology. They are semioval to subtriangular in outline and have slightly transversely concave posterior surfaces. In the proximal end of a more distal pedal phalanx, the proximal articular surface is subdivided into slightly asymmetrical concavities by a weakly developed medial ridge. Fragments of distal ends of pedal phalanges indicate strongly gynglimoidal articulations, with large and deep collateral ligament pits. Two partial pedal unguals are preserved. One is the ungual of the right pedal digit I (Fig. 9.3–4), which is preserved in approximately its life position with the distal ends of metatarsals II to IV. Its proximal end is damaged. The ungual is moderately curved, rather stout and has a single, ventrally placed claw groove on either side. As preserved, it is 35 mm long and 16 mm high and approximately 7 mm wide posteriorly. The dorsal surface is rounded. The other pedal ungual is only represented by its proximal end, which is 18 mm high and 10 mm wide. The proximal articular end is weakly subdivided by a vertical ridge, and a small flexor tubercle is present close to the proximal end. The dorsal margin of this ungual is sharp, and the cross-section asymmetrical, so that the claw groove is placed further dorsally on one side than on the other. This ungual might represent that of digit IV.

DISCUSSION

Systematic position of Pandoravenator

To test the systematic position of *Pandoravenator*, we included this taxon in three different phylogenetic matrices that includes a broad array of basal theropods. The first one is based on the matrix published by Carrano *et al.* (2012) with the subsequent modifications introduced by Rauhut *et al.* (2016). The second dataset is based on Smith *et al.* (2008) with the modifications introduced by Novas *et al.* (2015). The third dataset is that published by Rauhut (2003). We chose these matrices to establish the general affinities of the new taxon within the major clades of Theropoda, since they include a broad range of taxa and representatives of the major theropodan subclades rather than being focused on a specific subclade (*e.g.*, Benson *et al.*, 2010; Brusatte *et al.*, 2010; Pol and Rauhut, 2012; Loewen *et al.*, 2013). The character scorings of *Pandoravenator* for these three data matrices are given in the Appendix. The data matrices were analyzed in TNT v. 1.1 (Goloboff *et al.*, 2008) using equally weighted parsimony and the character ordering settings used in the original analyses.

The results of the three different phylogenetic analyses place *Pandoravenator* basally within Tentanurae. The specific positions retrieved for the new taxon within Tetanurae vary (Fig. 10), which is expected, based on its fragmentary nature and the different taxon and character sampling regimes of the three datasets. Nonetheless, our goal was to test the affinity of *Pandoravenator* with tetanurans, which is supported by multiple characters in the three phylogenetic analyses. The following list gathers the derived characters that support the inclusion of *Pandoravenator* in Tetanurae in the conducted phylogenetic analyses: mid caudal chevrons L-shaped (Rauhut, 2003: char. 130.1); large anterior process of chevron base (Novas *et al.*, 2015: char. 224.1); biceps tubercle of coracoid developed as a posteroventrally oriented ridge (Carrano *et al.*, 2012: char. 227.2; present in allosauroids); distal end of femur with an anteroposteriorly oriented trough separating lateral and medial convexities (Carrano *et al.*, 2012: char. 216.1; present in allosauroids and coelurosaurs); ridge on lateral side of tibia for connection

with fibula clearly separated from the proximal articular surface (Novas *et al.*, 2015: char. 358.2); ascending process of astragalus laminar (Carrano *et al.*, 2012: char. 331.1); astragalar condyles significantly expanded proximally on anterior side of tibia and face anterodistally (Rauhut, 2003: char. 217.1); astragalus proximal margin of the medial surface deeply concave anteroposteriorly in medial view (Novas *et al.*, 2015: char. 382.1; present also in abelisauroids); outline of proximal articular surface of metatarsal III hourglass-shaped (Novas *et al.*, 2015: char. 398.1); well-developed posteromedial flange on proximal end of metatarsal IV for articulation with metatarsal III (Novas *et al.*, 2015: char. 402.1).

As noted above, the position of *Pandoravenator* is restricted to basal nodes within Tetanurae (Fig. 10), given the presence of plesiomorphic features that are modified in more derived tetanurans, such as a rounded medial epicondyle of the femur (Carrano *et al.*, 2012: char. 310.0), distal extensor groove of femur absent (Novas *et al.*, 2015: char. 351.0; Carrano *et al.*, 2012: char. 311.0), and fibular condyle on proximal end of tibia confluent with cnemial crest anteriorly in proximal view (Rauhut, 2003: char. 204.0).

Pandoravenator *and its implications for the evolution of the tetanuran tarsus*

One of the unusual features of *Pandoravenator* is the morphology of the proximal tarsals. The taxon differs from all other theropods in the development of two notable tubercles on the astragalus at the junction with the calcaneum (Fig. 7). One of these is semicircular and placed directly below the contact of the astragalus with the anteromedial flange of the fibula, whereas the other is found on the dis-

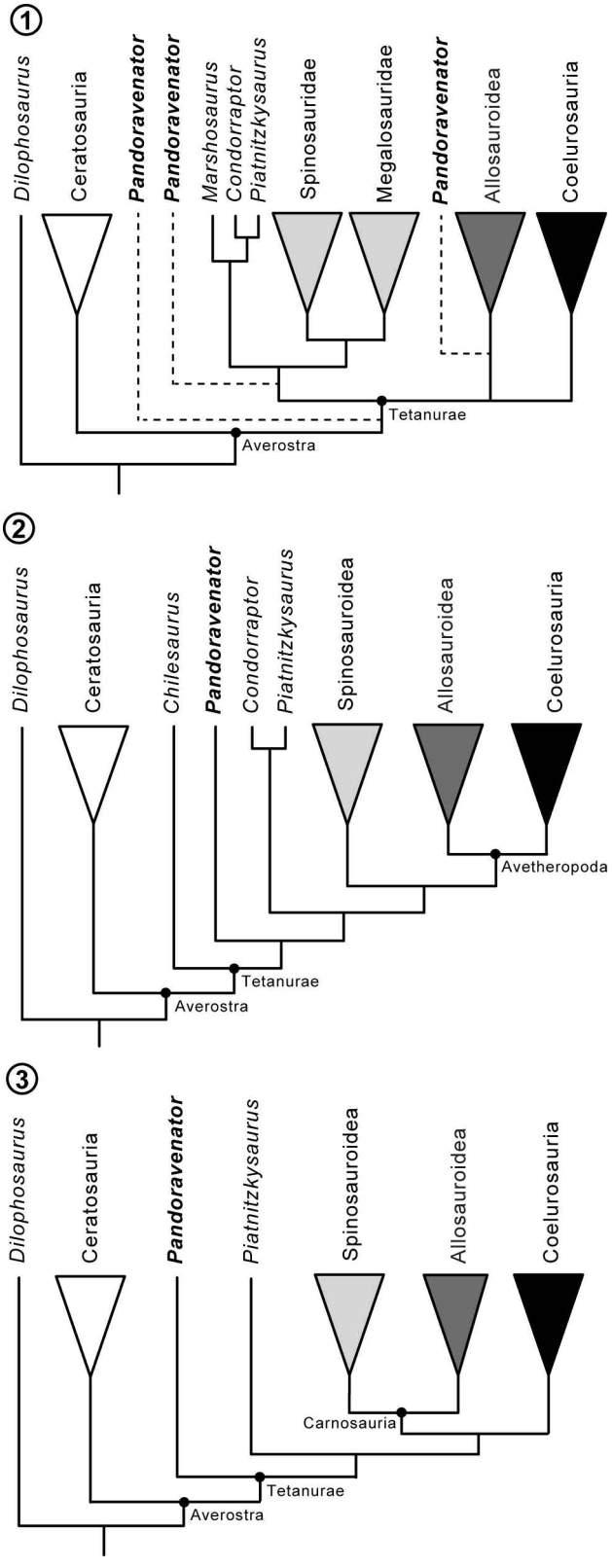

Figure 10. Phylogenetic positions of ***Pandoravenator fernandezorum*** in the three phylogenetic data matrices used in this study. The trees represent summarized consensus trees collapsing major clades of averostran theropods. **1,** phylogenetic results using the dataset of Rauhut *et al.* (2016), based on Carrano *et al.* (2012); dashed lines represent the alternative positions retrieved for ***Pandoravenator*** in the most parsimonious trees, allied to different basal nodes of Tetanurae (results based on reduced strict consensus); **2,** phylogenetic results using the dataset of Novas *et al.* (2015), based on Smith *et al.* (2008); **3,** phylogenetic results using the dataset of Rauhut (2003).

tal surface of the bone and seems to be triangular, although it is not completely preserved. These tubercles probably articulated with distal tarsal IV and, maybe, the lateral edge of distal tarsal II. Their functional significance is unclear, but these structures have not been described in the literature or observed by the authors in any other theropod, and are thus regarded as autapomorphies of *Pandoravenator*.

Origins of tetanuran apomorphies in the tibia and astragalus

In basal theropods the ascending process of the astragalus is usually placed on the lateral half of the bone, with a well-developed shelf for the reception of the distal end of the fibula lateral to it. The process itself is triangular in outline, usually with a vertical lateral border and gradually rising proximolaterally (see Welles and Long, 1974; Ezcurra and Novas, 2007). In proximal view, the process is blocky, its anteroposterior width reaching approximately half of the width of the astragalus laterally, and its posterolateral corner is connected to the posterior margin of the bone by an oblique ridge that marks the border between the tibial and fibular facets (*e.g.*, Huene, 1934: pl. 15, fig. 17). The distal part of the tibia is quadrangular to rectangular in outline and has a deep slot anterolaterally into which the ascending process of the astragalus fits (see Ezcurra and Novas, 2007).

In basal tetanurans, in contrast, the distal end of the tibia is relatively broader and triangular in outline, and the anterolateral notch is reduced to a narrow, oblique shelf on the anterior side of the distal end of the bone (see Rauhut, 2003: figs. 44–45). The ascending process of the astragalus is anteroposteriorly reduced, so that it forms a thin lamina of bone that overlaps the anterior side of the distal part of the tibia and contacts the distal part of the fibula with its usually slightly thickened lateral edge. In basal tetanurans, the ascending process is triangular to lobular in outline in anterior view and extends further laterally than in basal theropods, so that the facet for the fibula on the astragalar body is reduced and faces mainly laterally (*e.g.*, *Torvosaurus*, Britt, 1991; *Sinraptor*, Currie and Zhao, 1993, *Eustreptospondylus*, Sadleir *et al.*, 2008). Furthermore, the ascending process is relatively higher: *i.e.* as high as or higher than the astragalar body. The posterior ridge connecting the ascending process with the posterior rim of the astragalus is absent, as the expanded distal end of the tibia extends laterally onto the calcaneum. The astragalar body is also modified in tetanurans in comparison to basal theropods. The distal articular surface is extended anteriorly so that the articular surface for the distal tarsals and metatarsals faces anterodistally. A notable transverse groove transverses the articular condyles of the astragalus in most basal tetanurans (Welles and Long, 1974; Rauhut, 2003).

The situation in basal averostrans and ceratosaurs is variable, and thus the ancestral tetanuran condition is difficult to establish. The probably immediate outgroup taxon to averostrans, *Tachiraptor*, has only the distal end of the tibia preserved, and the morphology of its distal end was discussed by Langer *et al.* (2014). In the tibia of *Tachiraptor*, the notch in the anterolateral end of the distal part of the tibia is reduced in width and approaches the condition of the shelf on the anterior surface of the distal part of the tibia in tetanurans. Furthermore, the tibia is transversely expanded, with an especially expanded lateral malleolus, resulting in a roughly parallelogram-shaped outline that is considerably wider transversely than deep anteroposteriorly. In basal ceratosaurs, the situation is notably different in *Elaphrosaurus* and *Ceratosaurus*, two of the taxa for which the tibia and astragalus are known. In *Ceratosaurus*, the situation is furthermore complicated by the fact that the astragalus and calcaneum are fused to one another and preserved in articulation, if not fused with the tibia (Gilmore, 1920; Madsen and Welles, 2000). Nevertheless, the morphology of the distal part of the tibia in this taxon seems to be similar to the tetanuran condition, in that it is considerably expanded transversely and triangular in distal outline, with a stout, oblique shelf on the anterior side that extends over approximately half the width of the bone. However, the astragalus has a more transitional morphology. Although the expanded tibia extends laterally onto the calcaneum and the ascending process is laminar rather than blocky, the latter is low, triangular and has a well-developed facet laterally for the reception of the fibula. Furthermore, the distal condyles are mainly distally directed, with a very limited overlap onto the anterior side of the distal end of the tibia (Madsen and Welles, 2000). In *Elaphrosaurus*, the distal part of the tibia is strongly expanded transversely and broadly triangular in distal outline (Janensch, 1925; Rauhut and Carrano, 2016). The anterior side of the distal end is flat and lacks an oblique

shelf, thus resembling the condition in coelurosaurs and some derived abelisauroids (Rauhut, 2003, 2012). As in *Ceratosaurus*, the astragalar condyles are oriented distally and the ascending process is very low and transversely narrow (MB R 4960; Rauhut and Carrano, 2016).

The morphology of the distal part of the tibia and tarsus in *Pandoravenator* fits well in this general panorama, especially if this taxon represents one of the most basal tetanurans (*e.g.*, Fig. 10.2–3). The distal part of the tibia of *Pandoravenator* is broad and triangular in distal outline, but has a robust oblique shelf that extends to approximately half of the width of the distal end, similar to the condition in *Ceratosaurus* (Madsen and Welles, 2000). Likewise, the ascending process of the astragalus is laminar, but remarkably low and triangular in outline, pointing proximolaterally. However, in contrast to ceratosaurs (including *Ceratosaurus*), the distal condyles overlap the anterior surface of the distal part of the tibia so that the condyles are anterodistally directed, as in all tetanurans. Thus, *Pandoravenator* shows a novel combination of characters that may represent a transitional morphology in the evolution from the basal theropod tarsus to the modified tetanuran condition. The tarsus of *Pandoravenator* suggests that the extension of the astragalar condyles onto the anterior surface of the tibia (and the consequent functional changes in the mesometatarsal articulation) preceded the development of the high ascending astragalar process in the evolution of Tetanurae.

Astragalus ascending process as a separate ossification

A feature of special interest in the astragalus of *Pandoravenator* is the presence of a deep and continuous groove along the ventral end of the anteroproximal expansion of the distal condyles in the right element (Figs. 7.2, 11). Extant paleognath birds have a broad ascending process connected to the astragalus that resemble the condition of non-avian theropods (McGowan, 1985), whereas neognath birds have a "pretibial bone" that ossifies as a proximal projection of the calcaneum (Martin *et al.*, 1980). The homology of these structures and the astragalar ascending process of non-avian theropods have been controversially discussed in the 1980's and embryological information led to alternative interpretations. Some studies argued that these two processes originate from cartilaginous projections of the astragalus in all birds (McGowan, 1984, 1985), whereas others interpreted the "pretibial bone" as a development from a neomorphic cartilaginous precursor separated from the astragalus and calcaneum in neognaths (Martin *et al.*, 1980; Martin and Stewart, 1985). Ossa-Fuentes *et al.* (2015) have recently clarified the early cartilaginous development in birds and indicated that the ascending process of both paleognath and neognath birds originates from the primordial cartilagenous intermedium. Ossa-Fuentes *et al.* (2015) showed that birds have a developmental pathway unseen in other amniotes, in that the cartilaginous intermedium first expands proximally along the distal part of the tibia as the ascending process and later fuses with the tibiale (condylar region of astragalus) and calcaneum to form a single large cartilaginous cap for the tibia.

Although Ossa-Fuentes *et al.* (2015) have clarified the developmental decoupling of the intermedium from the astragalus and even noted that a separate ossification may have been present already in enanthiornithines, a major pending question is when this unique process appeared in the evolution of the lineage to birds. As noted by these authors, the decoupling event may have occurred as early as in dinosauriforms, but data from unfused tarsal elements is scarce among non-avian dinosaurs. Within theropods, previous reports (Welles, 1983) on a suture between the ascending process and the astragalar body in the basal theropod *Dilophosaurus* have been reconsidered and the alleged suture line cannot be distinguished from other multiple breaks in the astragalus of this taxon (Ossa-Fuentes *et al.*, 2015). On the other hand, the highly unusual tarsus of the heterodontosaurid *Fruitadens* shows a small separate ossification at the proximal end of the ascending process of the astragalus (Butler *et al.*, 2012), but the unusual morphology of the tarsus in general and the position of the separate ossification make its homology with the avian condition questionable (Ossa-Fuentes *et al.*, 2015).

The tarsus of *Pandoravenator* provides additional evidence on the homology of the tarsal structures in birds and non-avian theropods and has thus implications for our understanding of the evolution of the theropodan tarsus. We interpret the very conspicuous groove on the anterior side of the right astragalus of *Pandoravenator* as the remnants of a suture between two different centers of ossification. Assuming the homology of the separate ascending process

of *Pandoravenator* with the intermedium of birds that ossifies into the ascending process in these animals (Ossa-Fuentes *et al.*, 2015), this discovery thus presents the first direct evidence that supports the appearance of the unique bird developmental pathway at least in basal tetanurans, much earlier than the origin of birds.

Interestingly, an at least partial and usually shallow groove across the anterior side of the astragalar condyles is found in several ceratosaurs and many basal tetanurans (Welles and Long, 1974; Rauhut, 2003). This groove often coincides roughly with the boundary between the main astragalar body and the anteroproximal expansion of the astragalar condyles, even in cases where the latter is very restricted in its expansion, as in the ceratosaur *Ceratosaurus* (Madsen and Welles, 2000). In basal tetanurans the groove also extends across the anteroproximal expansion of the astragalar condyles (*e.g.*, *Allosaurus*, *Magnosaurus*, *Torvosaurus*, sinraptorids; Rauhut, 2003: p. 122) and is sometimes noted as a notch between the distal astragalar body and the anteroproximal expansion of the bone, closely comparable in position to the probable suture seen in *Pandoravenator* (Fig. 11). *Pandoravenator* helps interpreting the groove commonly found in ceratosarus and basal tetanurans as a remnant of the suture between two different centers of ossification in the theropod astragalus, likely representing the separate ossifications of the tibial cartilage as the astragalar body and the intermedium as the ascending process described for birds (Ossa-Fuentes *et al.*, 2015). The horizontal groove has been found as a probable averostran synapomorphy (*e.g.*, Rauhut, 2003; Carrano and Sampson, 2008) and is correlated with other changes of the tarsal joint in these animals, such as the lateral expansion of the distal part of the tibia to back the distal fibula and articulate with the calcaneum and the change from a rather massive, pyramidal ascending process to a sheet-like ascending process of the astragalus. These changes probably imply significant modifications in theropod locomotion from non-averostran to averostrans, but functional and biomechanical details about this apparently major change still need to be studied.

It is also interesting to note that coelurosaurs lack the groove across the anteroproximal expansion of the astragalar condyles described above, but bear a more proximally located discontinuous groove between the convex condyles and the laminar ascending process, which has been noted for many coelurosaur groups, including *Archaeopteryx* and basal birds (Mayr *et al.*, 2007; Chiappe *et al.*, 2007). Based on the variation of the proximodistal and lateromedial extension of the intermedium cartilage among extant birds (Ossa-Fuentes *et al.*, 2015: suppl. fig. 2), the condition of coelurosaurs may thus represent a proximal shift of the boundary between the tibial and the intermedium cartilages.

Figure 11. Left astragali in medial view. **1,** ***Pandoravenator fernandezorum*****, MPEF PV** 1733-36b. **2,** ***Allosaurus fragilis*****, MOR** 693. Abbreviations: **asc,** ascending process; **no,** notch. Scale bars= 10 mm.

CONCLUSIONS

The remains described here represent the first theropod for the Cañadón Calcáreo Formation fauna, a Late Jurassic assemblage previously represented by diplodocoid and macronarian neosauropods, basal crocodylomorphs, and coccolepid and basal teleosts fishes. As such, it is also the first representative of this clade from the Late Jurassic of Argentina in general. *Pandoravenator* contributes to the so far limited knowledge on the Late Jurassic theropod assemblages from Gondwana, until now restricted to the ceratosaurs and basal tetanurans of the Tendaguru Formation (Tanzania) and the bizarre *Chilesaurus* from the Toqui Formation (Chile). The Tendaguru Formation records are so far the most diverse, and the tetanurans and ceratosaurs from this unit have been interpreted as indicating a theropod fauna more similar to those from the Cretaceous of Gondwanan than to other Late Jurassic theropod faunas from the northern hemisphere (Rauhut, 2011). The thero-

pod records from the Late Jurassic of South America do not provide evidence either in favor nor contradicting this biogeographical scenario. In the case of *Chilesaurus*, interpreted as a basal tetanuran by Novas *et al.* (2015), its bizarre morphology is so autapomorphic that is hard to find particular affinities with other theropod species. In the case of *Pandoravenator*, it probably represents a basal branch of Tetanurae, but the fragmentary nature of the known remains precludes a more precise assessment of its phylogenetic affinities.

The significance of *Pandoravenator*, instead, relies more on its information regarding the evolution of a set of particular features that characterize the averostran or tetanuran tarsus. The morphology of the distal part of its tibia and proximal tarsals has a combination of plesiomorphies and apomorphies that sheds light on the origin of the tetanuran tarsus. Plesiomorphies include the presence of a relatively deep shelf along half of the anterior surface of the distal part of the tibia and a low and triangular ascending process of the astragalus, resembling the condition of some ceratosaurs. Tetanuran apomorphies include the extension of the articular surface of the astragalus onto the anterior surface of the distal part of the tibia and a triangular outline of the distal margin of the bone.

Finally, the ascending process of the astragalus of *Pandoravenator* has a deep and continuous groove across the anterior surface of the astragalar condyles that is interpreted as a sutural contact between two centers of ossification that would form the astragalus. This resembles the two centers of ossification recognized in the astragalus of extant birds and leads us to interpret a similarly located groove in ceratosaurs and non-coelurosaur tetanurans as a possible remnant of a suture. This interpretation implies that the unique developmental pattern seen in the astragalus of extant birds arose at least at the base of Averostra, which provides a minimum age for the event of developmental decoupling of the intermedium from the astragalus in the late Early Jurassic when the ceratosaur and tetanuran lineages diverged from one another.

ACKNOWLEDGEMENTS

Fieldwork and research were funded by DFG RA1012/9-1 and RA 1012/18-1 (to O.W.M.R.), ANPCyT PICT 0808 and 1288 (to D.P.), and by the Fundación Egidio Feruglio. Thanks are due to the participants of the 2002, 2009 and 2017 Jurassic expeditions. We thank L. Austin who conducted all illustrations and took most photographs used in this work. Critical comments by the editors, as well as M. Ezcurra, J. Choiniere, and A. Otero greatly helped to improve the manuscript. We also thank the Secretaría de Cultura de la Provincia del Chubut for granting permits to conduct fieldwork.

REFERENCES

Baron, M.G., and Barrett, P.M. 2017. A dinosaur missing-link? *Chilesaurus* and the early evolution of ornithischian dinosaurs. *Biology Letters* 13: 20170220.

Benson, R.B.J. 2010. A description of *Megalosaurus bucklandii* (Dinosauria: Theropoda) from the Bathonian of the UK and the relationships of Middle Jurassic theropods. *Zoological Journal of the Linnean Society* 158: 882–935.

Benson, R.B.J., Carrano, M.T., and Brusatte, S.L. 2010. A new clade of archaic large-bodied predatory dinosaurs (Theropoda: Allosauroidea) that survived to the latest Mesozoic. *Naturwissenschaften* 97: 71–78.

Bocchino, A. 1967. *Luisiella inexcutata* gen. et. sp. nov. (Pisces, Clupeiformes, Dussumieridae) del Jurâsico superior de la Provincia de Chubut, Argentina. *Ameghiniana* 4: 91–100.

Bonaparte, J.F. 1986. Les Dinosaures (Carnosaures, Allosauridés, Sauropodes, Cétiosauridés) du Jurassique moyen de Cerro Cóndor (Chubut, Argentine). *Annales de Paléontologie* 72: 247–289, 326–386.

Bordas, A.F. 1943. Peces del Cretácico del Río Chubut (Patagonia). *Physis* 19: 313–318.

Britt, B.B. 1991. Theropods of Dry Mesa Quarry (Morrison Formation, Late Jurassic), Colorado, with emphasis on the osteology of *Torvosaurus tanneri*. *BYU Geology Studies* 37: 1–72.

Brochu, C.A. 2003. Osteology of *Tyrannosaurus rex*: insights from a nearly complete skeleton and high-resolution computed tomographic analysis of the skull. *Society of Vertebrate Paleontology Memoir* 7: 1–138.

Brusatte, S.L., Carr, T.D., and Norell, M.A. 2012. The osteology of *Alioramus*, a gracile and long-snouted tyrannosaurid (Dinosauria: Theropoda) from the Late Cretaceous of Mongolia. *Bulletin of the American Museum of Natural History* 366: 1–197.

Brusatte, S.L., Norell, M.A., Carr, T.D., Erickson, G.M., Hutchinson, J.R., Balanoff, A.M., Bever, G.S., Choiniere, J.N., Makovicky, P.J., and Xu, X. 2010. Tyrannosaur paleobiology: new research on ancient exemplar organisms. *Science* 329: 1481–1485.

Brusatte, S.L., and Sereno, P.C. 2008. Phylogeny of Allosauroidea (Dinosauria: Theropoda): comparative analysis and resolution. *Journal of Systematic Palaeontology* 6: 155–182.

Butler, R.J., Porro, L.B., Galton, P.M., and Chiappe, L.M. 2012. Anatomy and cranial functional morphology of the small-bodied dinosaur *Fruitadens haagarorum* from the Upper Jurassic of the USA. *PLoS ONE* 7: e31556.

Cabaleri, N.G., Volkheimer, W., Armella, C., Gallego, O., Silva Nieto, D., Páez, M., Cagnoni, M., Ramos, A., Paranello, H., and Koukharsky, M. 2010. Estratigrafía, análisis de facies y paleoambientes de la Formación Cañadón Asfalto en el depocentro jurásico Cerro Cóndor, provincia del Chubut. *Revista de la Asociación Geológica Argentina* 66: 349–367.

Carballido, J.L., Rauhut, O.W.M., Pol, D., and Salgado, L. 2011. Osteology and phylogenetic relationships of *Tehuelchesaurus benitezii* (Dinosauria, Sauropoda) from the Upper Jurassic of Patagonia. *Zoological Journal of the Linnean Society* 163: 605–662.

Carrano, M.T. 2007. The appendicular skeleton of *Majungasaurus crenatissimus* (Theropoda: Abelisauridae) from the Late Cretaceous of Madagascar. *Society of Vertebrate Paleontology, Memoir*

8: 163–179.

Carrano, M.T., Benson, R.B.J., and Sampson, S.D. 2012. The phylogeny of Tetanurae (Dinosauria: Theropoda). *Journal of Systematic Palaeontology* 10: 211–300.

Carrano, M.T., and Sampson, S.D. 2008. The phylogeny of Ceratosauria (Dinosauria: Theropoda). *Journal of Systematic Palaeontology* 6: 183–236.

Carrano, M.T., Sampson, S.D., and Forster, C.A. 2002. The osteology of *Masiakasaurus knopfleri*, a small abelisauroid (Dinosauria: Theropoda) from the Late Cretaceous of Madagascar. *Journal of Vertebrate Paleontology* 22: 510–534.

Chiappe, L.M., Ji, S.A., and Ji, Q. 2007. Juvenile birds from the Early Cretaceous of China: Implications for enantiornithine ontogeny. *American Museum Novitates* 3594: 1–46.

Choiniere, J.N., Xu, X., Clark, J.M., Forster, C.A., Guo, Y., and Han, F. 2010. A basal alvarezsauroid theropod from the early Late Jurassic of Xinjiang, China. *Science* 327: 571–574.

Cúneo, R., Ramezani, J., Scasso, R.A., Pol, D., Escapa, I.H., Zavattieri, A.M., and Bowring, S.A. 2013. High-precision U–Pb geochronology and a new chronostratigraphy for the Cañadón Asfalto Basin, Chubut, central Patagonia: Implications for terrestrial faunal and floral evolution in Jurassic. *Gondwana Research* 24: 1267–1275.

Currie, P.J., and Zhao, X.J. 1993. A new carnosaur (Dinosauria, Theropoda) from the Jurassic of Xinjiang, People's Republic of China. *Canadian Journal of Earth Sciences* 30: 2037–2081.

Ezcurra, M.D., and Brusatte, S.L. 2011. Taxonomic and phylogenetic reassessment of the early neotheropod dinosaur *Camposaurus arizonensis* from the Late Triassic of North America. *Palaeontology* 54: 763–772.

Ezcurra, M.D., and Novas, F.E. 2007. Phylogenetic relationships of the Triassic theropod *Zupaysaurus rougieri* from NW Argentina. *Historical Biology* 19: 35–72.

Figari, E.G. 2005. [*Evolución tectónica de la cuenca de Cañadón Asfalto (Zona del valle medio del Río Chubut)*. Tesis Doctoral, Facultad de Ciencias Exactas y Naturales, Universidad de Buenos Aires, Buenos Aires, 177 p. Unpublished.].

Figari, E.G., and Courtade, S.F. 1993. Evolución tectosedimentaria de la Cuenca de Cañadón Asfalto, Chubut, Argentina. *XII Congreso Geológico Argentino y II Congreso de Exploración de Hidrocarburos* (Mendoza)*, Actas* 1: 66–77.

Figari, E.G., Scasso, R.A., Cúneo, R.N., and Escapa, I. 2015. Estratigrafía y evolución geológica de la Cuenca de Cañadón Asfalto, Provincia del Chubut, Argentina. *Latin American Journal of Sedimentology and Basin Analysis* 22: 135–169.

Gallego, O.F., Cabaleri, N.G., Armella, C., Volkheimer, W., Ballent, S.C., Martínez, S., Monferran, M.D., Silva Nieto, D.G., and Páez, M.A. 2011. Paleontology, sedimentology and paleoenvironment of a new fossiliferous locality of the Jurassic Cañadón Asfalto Formation, Chubut Province, Argentina. *Journal of South American Earth Sciences* 31: 54–68.

Gauthier, J.A. 1986. Saurischian monophyly and the origin of birds. *Memoirs of the Californian Academy of Science* 8: 1–55.

Gilmore, C.W. 1920. Osteology of the carnivorous Dinosauria in the United States National Museum, with special reference to the genera *Antrodemus* (*Allosaurus*) and *Ceratosaurus*. *Bulletin of the United States National Museum* 110: 1–154.

Goloboff, P.A., Farris, J.S., and Nixon, K. 2008. TNT, a free program for phylogenetic analysis. *Cladistics* 24: 774–786.

Huene, F.v. 1934. Ein neuer Coelurosaurier in der thüringschen Trias. *Palaeontologische Zeitschrift* 16: 145–168.

Janensch, W. 1920. Ueber *Elaphrosaurus bambergi* und die Megalosaurier aus den Tendaguru-Schichten Deutsch-Ostafrikas. *Sitzungsberichte der Gesellschaft naturforschender Freunde zu Berlin* 1920: 225–235.

Janensch, W. 1925. Die Coelurosaurier und Theropoden der Tendaguru-Schichten Deutsch-Ostafrikas. *Palaeontographica Supplement* 7 1: 1–99.

Janensch, W. 1929. Ein aufgestelltes und rekonstruiertes Skelett von *Elaphrosaurus bambergi*. Mit einem Nachtrag zur Osteologie dieses Coelurosauriers. *Palaeontographica Supplement* 7 1: 279–286.

Kobayashi, Y., and Barsbold, R. 2005. Reexamination of a primitive ornithomimosaur, *Garudimimus brevipes* Barsbold, 1981 (Dinosauria: Theropoda), from the Late Cretaceous of Mongolia. *Canadian Journal of Earth Sciences* 42: 1501–1521.

Lambe, L.M. 1917. The Cretaceous theropodous dinosaur *Gorgosaurus*. *Canada Department of Mines, Geological Survey, Memoir* 100: 1–84.

Langer, M.C., Rincón, A.D., Ramezani, J., Solórzano, A., and Rauhut, O.W.M. 2014. New dinosaur (Theropoda, stem-Averostra) from the earliest Jurassic of the La Quinta formation, Venezuelan Andes. *Royal Society Open Science* 1: 140184.

Loewen, M.A., Irmis, R.B., Sertich, J.J.W., Currie, P.J., and Sampson, S.D. 2013. Tyrant dinosaur evolution tracks the rise and fall of Late Cretaceous oceans. *PLoS ONE* 8: e79420.

López-Arbarello, A., Rauhut, O.W.M., and Moser, K. 2008. Jurassic fishes of Gondwana. *Revista de la Asociación Geológica Argentina* 63: 586–612.

López-Arbarello, A., Sferco, M.E., and Rauhut, O.W.M. 2013. A new genus of coccolepidid fishes (Actinopterygii, Chondrostei) from the continental Jurassic of Patagonia. *Palaeontologia Electronica* 16: 1–23.

Madsen, J.H.Jr. 1976. *Allosaurus fragilis*: a revised osteology. *Utah Geological and Mineralogical Survey Bulletin* 109: 3–163.

Madsen, J.H.Jr., and Welles, S.P. 2000. *Ceratosaurus* (Dinosauria, Theropoda). A revised osteology. *Miscellaneous Publication, Utah Geological Survey* 00-2: 1–80.

Marsh, O.C. 1881. Principal characters of American Jurassic dinosaurs. Part V. *American Journal of Science (ser. 3)* 21: 417–423.

Martin, L.D., and Stewart, J.D. 1985. Homologies in the avian tarsus. *Nature* 315: 159–160.

Martin, L.D., Stewart, J.D., and Whetstone, K.N. 1980. The origin of birds: structure of the tarsus and teeth. *The Auk* 97: 86–93.

Mayr, G., Pohl, B., Hartman, S., and Peters, S. 2007. The tenth skeletal specimen of *Archaeopteryx*. *Zoological Journal of the Linnean Society* 149: 97–116.

McGowan, C. 1984. Evolutionary relationships of ratites and carinates: evidence from ontogeny of the tarsus. *Nature* 307: 733–735.

McGowan, C. 1985. Tarsal development in birds: evidence for homology with the theropod condition. *Journal of Zoology (A)* 206: 53–67.

Nesbitt, S.J., and Ezcurra, M. 2015. The early fossil record of dinosaurs in North America: A new neotheropod from the base of the Upper Triassic Dockum Group of Texas. *Acta Palaeontologica Polonica* 60: 513–526.

Norell, M.A., and Makovicky, P.J. 1999. Important features of the dromaeosaur skeleton II: Information from newly collected specimens of *Velociraptor mongoliensis*. *American Museum Novitates* 3282: 1–45.

Novas, F.E., Salgado, L., Suárez, M., Agnolín, F.L., Ezcurra, M.D., Chimento, N.R., de La Cruz, R., Isasi, M.P., Vargas, A.O., and Rubilar-Rogers, D. 2015. An enigmatic plant-eating theropod from the Late Jurassic period of Chile. *Nature* 522: 331–334.

O'Connor, P.M. 2007. The postcranial axial skeleton of *Majun-*

gasaurus crenatissimus (Theropoda: Abelisauridae) from the Late Cretaceous of Madagascar. *Society of Vertebrate Paleontology Memoir* 8: 127–162.

Osmólska, H., Roniewicz, E., and Barsbold, R. 1972. A new dinosaur, *Gallimimus bullatus* n. gen., n. sp. (Ornithomimidae) from the Upper Cretaceous of Mongolia. *Palaeontologia Polonica* 27: 103–143.

Ossa-Fuentes, L., Mpodozis, J., and Vargas, A.O. 2015. Bird embryos uncover homology and evolution of the dinosaur ankle. *Nature Communications* 6: 8902.

Ostrom, J. 1969. Osteology of *Deinonychus antirrhopus*, an unusual theropod from the Lower Cretaceous of Montana. *Peabody Museum of Natural History Bulletin* 30: 1–165.

Owen, R. 1842. Report on British fossil reptiles. Part II. *Reports of the British Association for the Advancement of Sciences* 11: 60–204.

Padian, K. 1986. On the type material of *Coelophysis* Cope (Saurischia: Theropoda) and a new specimen from the Petrified Forest of Arizona (Late Triassic: Chinle Formation). In: K. Padian (Ed.), *The beginning of the age of dinosaurs*. Cambridge University Press, Cambridge, p. 45–60.

Pol, D., and Rauhut, O.W.M. 2012. A Middle Jurassic abelisaurid from Patagonia and the early diversification of theropod dinosaurs. *Proceedings of the Royal Society London B* 279: 3170–3175.

Pol, D., Rauhut, O.W.M., Lecuona, A., Leardi, J.M., Xu, X., and Clark, J.M. 2013. A new fossil from the Jurassic of Patagonia reveals the early basicranial evolution and the origins of Crocodyliformes. *Biological Reviews* 88: 862–872.

Raath, M.A. 1977. [*The anatomy of the Triassic theropod Syntarsus rhodesiensis (Saurischia: Podokesauridae) and a consideration of its Biology*. PhD thesis, Rhodes University, Grahamstown, 233 p. Unpublished.].

Rauhut, O.W.M. 2003. The interrelationships and evolution of basal theropod dinosaurs. *Special Papers in Palaeontology* 69: 1–213.

Rauhut, O.W.M. 2005a. Postcranial remains of "coelurosaurs" (Dinosauria, Theropoda) from the Late Jurassic of Tanzania. *Geological Magazine* 142: 97–107.

Rauhut, O.W.M. 2005b. Osteology and relationships of a new theropod dinosaur from the Middle Jurassic of Patagonia. *Palaeontology* 48: 87–110.

Rauhut, O.W.M. 2006. A brachiosaurid sauropod from the Late Jurassic Cañadón Calcáreo Formation of Chubut, Argentina. *Fossil Record* 9: 226–237.

Rauhut, O.W.M. 2011. Theropod dinosaurs from the Late Jurassic of Tendaguru (Tanzania). *Special Papers in Palaeontology* 86: 195–239.

Rauhut, O.W.M. 2012. A reappraisal of a putative record of abelisauroid theropod dinosaur from the Middle Jurassic of England. *Proceedings of the Geologists' Association* 123: 779–786.

Rauhut, O.W.M., Carballido, J.L., and Pol, D. 2015. A diplodocid sauropod dinosaur from the Late Jurassic Cañadón Calcáreo Formation of Chubut, Argentina. *Journal of Vertebrate Paleontology* 35: e982798.

Rauhut, O.W.M., and Carrano, M.T. 2016. The theropod dinosaur *Elaphrosaurus bambergi* Janensch, 1920, from the Late Jurassic of Tendaguru, Tanzania. *Zoological Journal of the Linnean Society* 178: 546–610.

Rauhut, O.W.M., Hübner, T.R., and Lanser, K.P. 2016. A new megalosaurid theropod dinosaur from the late Middle Jurassic (Callovian) of north-western Germany: Implications for theropod evolution and faunal turnover in the Jurassic. *Palaeontologia Electronica* 19.2.26A: 1–65.

Rauhut, O.W.M., and López-Arbarello, A. 2008. Archosaur evolution during the Jurassic: a southern perspective. *Revista de la Asociación Geológica Argentina* 63: 557–585.

Rauhut, O.W.M., Milner, A.C., and Moore-Fay, S.C. 2010. Cranial osteology and phylogenetic position of the theropod dinosaur *Proceratosaurus bradleyi* (Woodward, 1910) from the Middle Jurassic of England. *Zoological Journal of the Linnean Society* 158: 155–195.

Rauhut, O.W.M., Remes, K., Fechner, R., Cladera, G., and Puerta, P. 2005. Discovery of a short-necked sauropod dinosaur from the Late Jurassic period of Patagonia. *Nature* 435: 670–672.

Rauhut, O.W.M., and Xu, X. 2005. The small theropod dinosaurs *Tugulusaurus* and *Phaedrolosaurus* from the Early Cretaceous of Xinjiang, China. *Journal of Vertebrate Paleontology* 25: 107–118.

Rich, T.H., Vickers-Rich, P., Gimenez, O., Cúneo, R., Puerta, P., and Vacca, R. 1999. A new sauropod dinosaur from Chubut Province, Argentina. *National Science Museum Monographs* 15: 61–84.

Rowe, T. 1989. A new species of the theropod dinosaur *Syntarsus* from the Early Jurassic Kayenta Formation of Arizona. *Journal of Vertebrate Paleontology* 9: 125–136.

Sadleir, R., Barrett, P.M., and Powell, H.P. 2008. The anatomy and systematics of *Eustreptospondylus oxoniensis*, a theropod dinosaur from the Middle Jurassic of Oxfordshire, England. *Monograph of the Palaeontographical Society* 160: 1–82.

Salgado, L., De La Cruz, R., Suárez, M., Fernández, M.S., Gasparini, Z., Palma-Heldt, S., and Fanning, M. 2008. First Late Jurassic dinosaur bones from Chile. *Journal of Vertebrate Paleontology* 28: 529–534.

Sferco, M.E. 2012. [*Filogenia y Biogeografía de los peces teleósteos (Actinopterygii, Teleostei) de la Formación Cañadón Calcáreo (Jurásico; Provincia del Chubut, Argentina).* Tesis Doctoral, Facultad de Ciencias Exactas y Naturales, Universidad de Buenos Aires, 386 p. Unpublished.].

Sferco, M.E., López-Arbarello, A., and Báez, A.M. 2015. Anatomical description and taxonomy of †*Luisiella feruglioi* (Bordas), new combination, a freshwater teleost (Actinopterygii, Teleostei) from the Upper Jurassic of Patagonia. *Journal of Vertebrate Paleontology* 35: e924958.

Smith, N.D., Makovicky, P.J., Agnolín, F.L., Ezcurra, M.D., Pais, D.F., and Salisbury, S.W. 2008. A *Megaraptor*-like theropod (Dinosauria: Tetanurae) in Australia: support for faunal exchange across eastern and western Gondwana in the Mid-Cretaceous. *Proceedings of the Royal Society London B* 275: 2085–2093.

Smith, N.D., Makovicky, P.J., Hammer, W.R., and Currie, P.J. 2007. Osteology of *Cryolophosaurus ellioti* (Dinosauria: Theropoda) from the Early Jurassic Antarctica and implications for early theropod evolution. *Zoological Journal of the Linnean Society* 151: 377–421.

Tykoski, R.S. 2005. [*Anatomy, ontogeny, and phylogeny of coelophysoid theropods.* PhD thesis, University of Texas, Austin, 553 p. Unpublished.].

Volkheimer, W., Quattrocchio, M.E., Cabaleri, N.G., Naváez, P.L., Rosenfeld, U., Scafati, L., and Melendi, D.L. 2015. Environmental and climatic proxies for the Cañadón Asfalto and Neuquén basins (Patagonia, Argentina): review of Middle to Upper Jurassic continental and near coastal sequences. *Revista Brasileira de Paleontologia* 18: 71–82.

Welles, S.P. 1983. Two centers of ossification in a theropod astragalus. *Journal of Paleontology* 57: 401.

Welles, S.P. 1984. *Dilophosaurus wetherilli* (Dinosauria, Theropoda) osteology and comparisons. *Palaeontographica Abt. A.* 185: 87–180.

Welles, S.P., and Long, R.A. 1974. The tarsus of theropod dinosaurs.

Annals of the South African Museum 64: 191–218.
Xu, X., Ma, Q., and Hu, D. 2010. Pre-*Archaeopteryx* coelurosaurian dinosaurs and their implications for understanding avian origins. *Chinese Science Bulletin* 55: 3971–3977.

doi: 10.5710/AMGH.12.10.2017.3105

Submitted: April 4th, 2017
Accepted: October 12th, 2017
Published online: November 1st, 2017

APPENDIX

The following scorings were used in the phylogenetic analyses for the three different data matrices.

Rauhut et al. (2016)

Pandoravenator

??
??
??
??
0?20????????00???
??????????????????????????????100001011000?20?000?01
100000??0?21?1??00???

Novas et al. (2015)

Pandoravenator

??
??
??
??0????
1??0?????????????10????????0????????????????????????????
??
???????????????000001??2?001?21?00000010001110010
01110?01????001000111?20?????

Rauhut (2003)

Pandoravenator

??
??
?????????1???0?101????1????????????????????????????????
? 1 1 0 1 [1
2]020?0000001010?[1 2]2?